Reflection-Analysis on Different Types of Light-Beams for Short Distances

Master‘s thesis

BSc. Krenar Sh. REXHEPI

Institute of Microwave and Photonic Engineering

Graz University of Technology

Supervisor: **Prof. Dr. Erich Leitgeb**

Assistant Advisor: **Dipl.-Ing. Pirmin Pezzei**

Graz, September 2014

Eid (Ehrenwörtliche Erklärung)

Ich erkläre an Eides Statt, dass ich die vorliegende Arbeit selbstständig und ohne fremde Hilfe verfasst, andere als die angegebenen Quellen nicht benutzt und die den benutzten Quellen wörtlich und inhaltlich entnommenen Stellen als solche kenntlich gemacht habe.

Ich versichere, dass ich dieses Diplomarbeitsthema bisher weder im In- noch im Ausland (einer Beurteilerin oder einem Beurteiler) in irgendeiner Form als Prüfungsarbeit vorgelegt habe.

Graz, September 2014 .....

Unterschrift

STATUTORY DECLARATION

I declare that I have authored this thesis independently, that I have not used other than the declared sources / resources and that I have explicitly marked all material which has been quoted either literally or by content from the used sources.

Graz, September 2014 .....

Signature

Acknowledgements

In the name of Allah the most Beneficent and the most Merciful, the one who rules all over the earth, heavens and everything that exists in between. All praise is to Allah for all His power, His blessings, His majesty, His sovereignty and everything related to Him, whether we know it or not. Peace and prayer be upon our beloved Prophet Muhammad (S.A.W), his family and all of his companions.

Acknowledgements are for my supervisor Prof. Dr. Erich Leitgeb and my assistant advisor DI. Pirmin Pezzei who supported me in all possible ways by giving his advice, encouragement and all required resources to accomplish the master's thesis. For correction of this work thanks are for Phd. Student H.N.Khan and DI. A.Kuleta. I am also thankful to my colleagues at institute of Microwave and Photonics Engineering who helped me giving me suggestions.

My heart is being filled with the sensation of thankfulness especially for my parents, sisters, friends and my well-wishers who prayed for my success and have remained the binding force in my life all through this work. I am highly grateful to my wife for her care, patience and support. Thanks are also for my best friend and also my roommate Chamy, who supported me in several ways during the studying. During the thesis many people have been supportive and deserve my heartiest gratitude. Thanks to anybody, I missed whosoever deserves a mention!

Graz, 2014 **BSc. Krenar Sh. REXHEPI**

Kurzfassung

Die Ausbreitung von Licht durch die Luft kann auf unterschiedliche Weise von Objekten in der Natur rück reflektiert (gespiegelt) werden. Die Materialoberfläche kann eine Reflexion wie ein Spiegel verursachen, aber auch diffuse Reflexion oder eine Kombination von beiden Fällen ist möglich. Für „Free Space Optics“ (FSO) Anwendungen ist es wichtig, die Wechselwirkung zwischen dem Lichtstrahl und der reflektierenden Oberfläche zu analysieren.

In dieser Masterarbeit werden einige Parameter untersucht, um die Intensität des reflektierten Gauß-verteilten Strahls bei Reflexion an verschiedenen Materialoberflächen (im Infrarotbereich 850 nm) zu berechnen und zu analysieren. Die Reflexionskoeffizienten von unterschiedlichen Materialien beeinflussen die Intensität der reflektierten Gauß-Strahlverteilung. Mit Matlab wird zuerst der Fall der Gauß-Strahlverteilung untersucht, wenn der Lichtstrahl auf der Zieloberfläche und zurück reflektiert wird. Zusätzlich werden andere Strahlverteilungen und Mehrfachreflexionen betrachtet und als letzter Teil eine Untersuchung mit mehreren optischen Quellen. Der Schwerpunkt der Arbeit ist die Analyse der Strahlverteilung und Reflexionen. Als Ergebnis erhält man analytische Berechnungen unter Betrachtung geometrischer Ausdrücke, die für „Optical Wireless Systeme“ Verwendung finden. Bei den untersuchten Strahlformen ist neben der Gauß-Verteilung auch die Betrachtung des Lambert Strahlers ein wesentlicher Faktor der analysierten Lichtintensitäten. Die Entfernung zwischen der verwendeten LD-Lichtquelle (Laserdiode, mit Leistung von 6 mW) und der Reflexionsfläche wird dabei mit 15 mm angegeben.

Abstract

Propagation of light through the air could be reflected in different ways from objects in the nature. The material surfaces may have a reflection as a mirror, diffuse or a combination of both (mirror and diffuse). In indoor Free Space Optics (FSO) it is important to analyze the interaction between light and reflecting surfaces.

In the framework of this research, some specifications are given to calculate the intensity of reflected Gaussian distribution beam on various material surfaces (in infrared region 850nm). The reflection coefficient from various materials affects the intensity of reflected Gaussian beam distribution. Using Matlab as a simulation tool, the Gaussian beam distribution (when the light beam hits the target surface and reflects back to the source surface) is simulated. Additional part of experimental work is beam distribution using multiple optical sources. Distance between the LD-source (6mW) and reflecting surface is 15mm. The main focus of this research is the analysis of optical beam with its reflections. As a result of it, analytical and geometrical expressions are presented. Lambertian beam distribution has also been investigated.

Contents

1. Introduction 1

1.1. Motivation 1
1.2. Related Work 2

2. Relevance of Reflectance on FSO 3

2.1. Methods for measuring the reflectivity 3
2.1.1. QTR-1A Reflectance Sensor 3
2.1.2. Loss Meter metrology instrument 4
2.2. Reflectivity of light on building materials 5
2.3. Channel Models for Radio on Visible (RoVL) Communication System 9
2.4. Other related projects 12
2.4.1. Model for indoor wireless optical link 12
2.4.2. Simulation of reflected and scattered laser radiation 12
2.4.3. The near infrared reflective material surfaces 12

3. Fundamentals 13

3.1. Indoor Free space optical propagation 14
3.2. Reflection and refraction 16
3.2.1. Reflection factors of an electrically transverse polarized wave 17
3.2.2 .Reflection factors of an magnetically transverse polarized wave 20
3.2.3. Reflectance and transmittance 26
3.3. Gaussian beam 27
3.3.1. Beam spreading 27
3.3.2. Intensity 29
3.4. Diffuse beam 32
3.4.1. Gaussian beam with a Light Shaping Diffuser (LSD) 32
3.4.2. Lambertian beam 35
3.5. Optical properties of materials 37

4. Investigations on Light-Beam using MATLAB® 38

4.1. Simulation of Gaussian beam distribution and mirror surface 38
4.1.1. Direct beam with single reflection and multiple reflections 39
4.1.2. Reflected beam and incident angle 43

4.1.3. Direct reflected beam and reflection coefficient 48
4.1.4. Reflected beam and beam width angles in x and y direction 49
4.2. Simulation of diffuse beam distribution 50
4.2.1. Comparison of the beam waist radius 51
4.2.2. Simulation of relative directional reflectivity (RDR) 53
4.2.3. Reflected diffuse beam distribution and scattering angle 54
4.2.4. Reflected diffuse beam distribution and reflection coefficient 55
4.2.5. Intensity of Lambertian beam distribution 56

5. Beam distribution with multiple sources 59

5.1. Beam distribution with four transmitters in 3D 59
5.2. Beam distribution with four transmitters 63
5.2.1. Beam distribution with four transmitters in y-direction 63
5.2.1. Beam distribution with four transmitters and angle of incidence 66
5.3. Beam distribution with eight transmitters 69

6. Results 71

7. Conclusion 73

Bibliography 74

List of Figures 78

List of Tables 82

List of Abbreviations 83

Appendix A 84

Appendix B 89

Appendix C 91

Appendix D 93

1. Introduction

Over 70% of the wireless voice and data traffic takes place in an indoor environment. Indoor wireless optical communication has its advantages, for example low-cost and high reliability. Visible light communications (VLC) has such a promise and exploits the existing illumination infrastructure (i.e., LEDs) for wireless communication purposes **[27]**.

1.1. Motivation

Optical fibers have advanced greatly over the last decade and become an important field of communication technology today. As an alternative to the optical networks is so called free space optical (FSO) network. In indoor environment (room, office etc.), optical beam propagates through the air (free space) to the receiver's side. Optical wireless link could be a directed one as Line-of-sight (LOS) or a diffuse (reflected from the walls) one.

The region of operation is in near-infrared (850 nm). Short distance between optical source and object is 15mm. The divergence angle of the beam is 20 degree. For the optical source, Gaussian and Lambertian beam distribution is used. Diffusion beam is also part of the experimental tasks.

This work is organized as follow. In chapter 2, introduction of several projects related to this work are explained. Chapter 3 shows the key theoretical aspects of the optical reflection in detail (reflection and refraction, Gaussian and diffuse beam distributions, and optical properties of materials). Chapter 4 demonstrates the simulation parts of this thesis. For the simulation, MATLAB® has been used. Experimental part of simulations continues in chapter 5, with beams distributions using multiple optical sources. Chapter 6 deals with results of the simulation tasks. Finally, chapter 7 gives a conclusion of my work and also the futuristic research possibilities.

1.2. Related work

Nowadays there are several research projects about optical reflection and its behavior with various materials. Instrumentation for the measurement of reflectance takes many forms **[10]**. The characterization of appearance of materials involves measurements of reflectance, both diffuse and specular. Numerous procedures and instruments have been devised for goniophotometry, the measurement of specular gloss with biconical geometry. Also, many papers have explained the instruments, methods, and procedures. Some of them are discussed in the next chapter.

2. Relevance of Reflectance on FSO

There are a lot of investigation projects on propagation of the light beam. The influence of reflectance on atmosphere is evident. Following sections mention measurements methods, instruments and also some research projects focusing on optical reflections.

2.1. Methods for measuring the reflectivity

In recent years, researchers have great interest on FSO using multiple various methods. The reflectance sensor and Loss Meter metrology instrument are demonstrated as measurement techniques for reflectivity.

2.1.1 QTR-1A Reflectance Sensor

An important measurement task is the reflection measurements of different surfaces using reflective optical object sensor for short distances QTR-1A Sensor. The reflective optical sensor consists of an invisible infrared light emitting diode (LED) as a transmitter source that operates with 950nm in continuous wave (CW) and a phototransistor as receiver. The phototransistor is connected to a pull-up resistor to form a voltage divider that produces an analog voltage output between 0 V and V_{IN} (which is typically 5 V) as a function of the reflected IR. Lower output voltage is an indication of a greater reflection **[30].**

Fig.1. QTR-1A Reflectance Sensor **[30]**

2.1.2. Loss Meter metrology instrument

The Loss Meter metrology instrument was developed for measuring high reflectivity/low loss optical components. The Loss Meter utilizes the cavity ring down (CRD) technique to measure the total optical loss associated with a test sample, and enables the total optical loss ranging from 0.001 to 0.000005 (1000 ppm to 5 ppm) to be determined with high precision. The system can be used for determining losses/reflectance in high reflectivity mirrors as well as losses due to absorption and scatter in thin films and thin/thick optical substrates. The system has been specifically developed and configured for ease-of-use by technicians, thus providing a valuable and in-house diagnostic for optics production facilities. Instruments may be configured as either fixed wavelength systems or tuneable, scanned systems in spectral regions ranging from the ultraviolet to middle infrared. Minimum instrument precision is typically less than 1% of the total measured loss, resulting in a precision better than 1 ppm for 100 ppm losses (R=99.99%) and 10 ppm for 1000 ppm losses (R=99.9%). Total optical loss/reflectance/absorption data of the test optic is updated in real-time at user-defined intervals **[32]**.

.

Fig.2. Loss Meter metrology instrument **[32]**

The Loss Meter metrology instrument is based on the cavity ring down (CRD) technique for measuring optical loss. In this technique an optical cavity is formed between two or more high-reflectivity mirrors. A light source is used to inject light into the cavity where it bounces back and forth between the high-

reflectivity end mirrors. Because the cavity mirrors are not 100 % reflective, some of the light leaks out with each reflection. Measured decay curve of a linear cavity from a CW-laser based Loss Meter system operating at 1315 nm. A portion of the pre-trigger signal is shown illustrating the relatively constant signal seen before the laser is turned off. Once the laser is turned off at t=0, the light within the cavity decays exponentially (see fig.3).

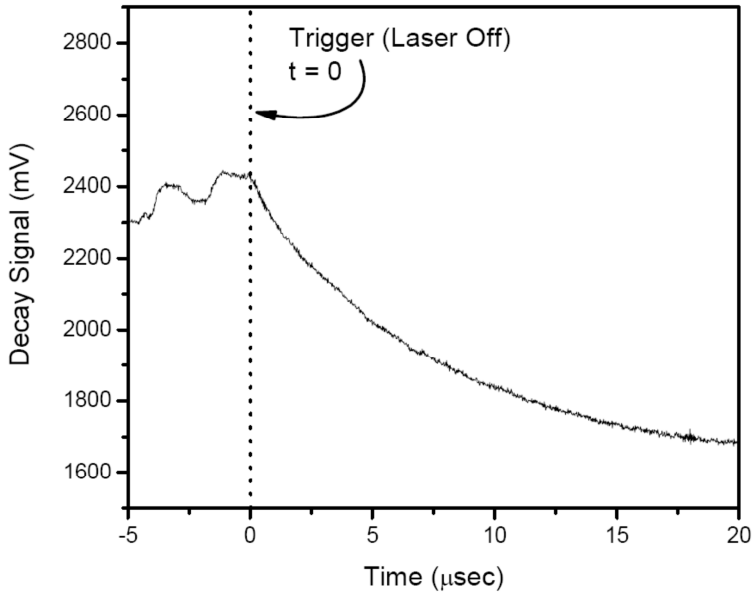

Fig.3. Decay curve of a linear cavity from a CW-laser (1315 nm) **[32]**

2.2. Reflectivity of light on building materials

Reflectivity of light on building materials describes the diffusion systems as an alternative to NLOS in indoor FSO. These systems are able to cover a larger area than NLOS. Reflection values of different samples from different materials in the 650nm and 850nm region are measured. The laser diode is connected to ThorLabs LDC 202 (Laser Diode Controller) and ThorLabs TED200 (temperature controller) for setting a constant optical output of 100 nW. The reflected optical beam (optical power 100 nW) of the sample is measured at different distances from the laser diode with an angle of rotation φ = 5°. Experimental measurements are performed in the range 0 - 180°. The position of the laser diode was 90° and 45° (see Fig.4) at wavelengths of 650 nm and 850 nm **[12]**.

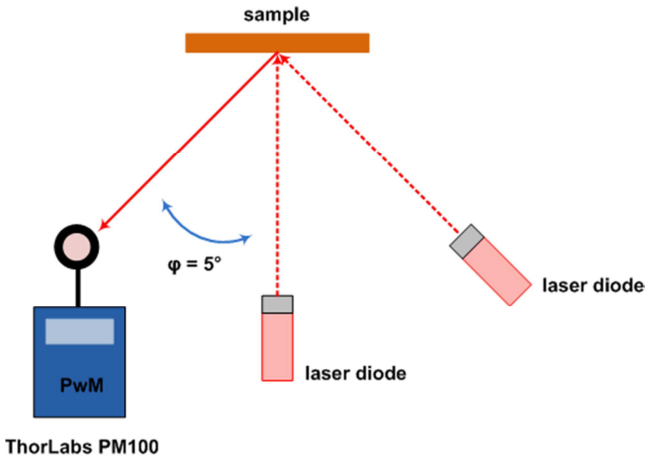

Fig.4. Block diagram of measuring system of directional characteristics **[12]**

For the experimental measurement of the directional characteristics of building materials, two groups of samples have been created. The first group consist of coatings which was two-times applied to the plaster. The second group includes samples of tiling, building and structural materials.

Fig.5.The samples of coatings **[12]**

1	ROKO – INTERIER SUPER RK 400
2	HET KLASIK COLOR
3	PRIMALEX PLUS
4	PRIMALEX BONUS
5	HETLINE
6	HET KLASIK
7	PRIMALEX STANDARD (tinting)
8	EXIN EKO
9	Paste for tinting
10	PRIMALEX STANDARD

Table 1.The description of samples of coatings **[12]**

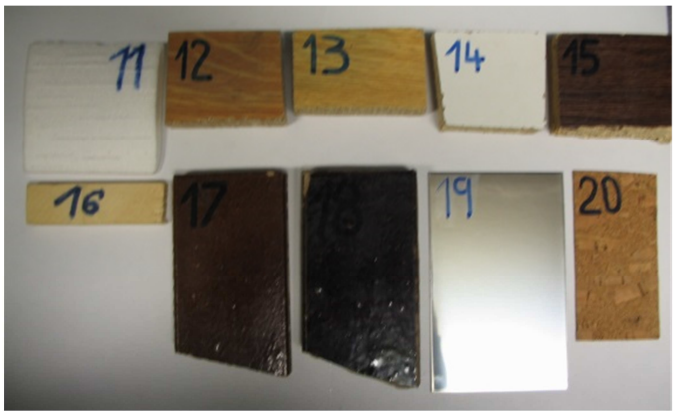

Fig.6.The samples of building and tiling materials **[12]**

11	POLYSTYREN
12	wooden board (light brown)
13	wooden board (ochre)
14	wooden board (white)
15	wooden board (dark brown)
16	spruce wood
17	clinker glossy (light brown)
18	clinker glossy (dark brown)
19	steel
20	cork

Table 2.The samples of building and tiling materials **[12]**

Examples of the measured values of direction characteristic are shown in fig.7 and fig.8. The measured values of sample no.13 show that the directional characteristic is combined (diffuse and directional diffuse) and in the case of sample no.6 directional characteristic is diffuse.

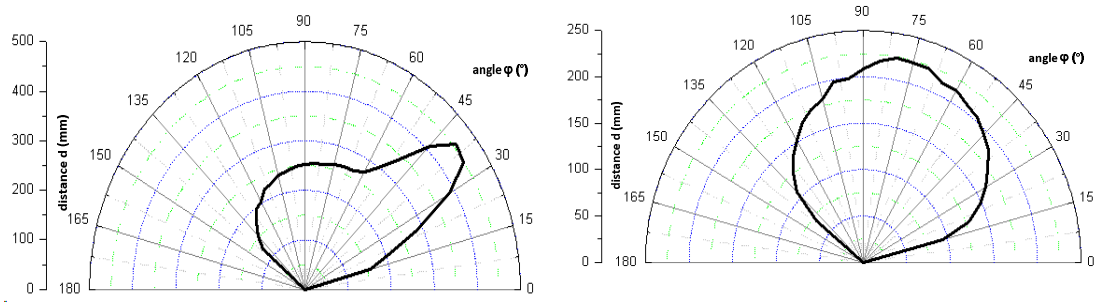

Fig.7.Directional characteristic of a) sample no.13 and b) no.6 (650 nm) **[12]**

The difference of the measured directional characteristics when using wavelength of 650 nm and 850 nm range is evident. The higher wavelength the larger covered area of reflected optical radiation (fig.7 and fig.8).

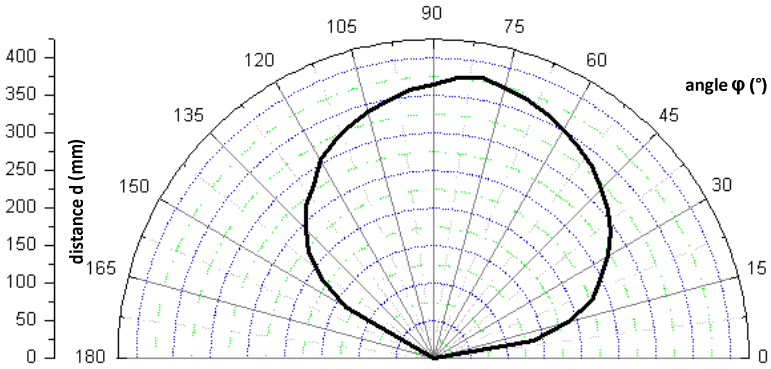

Fig.8.Directional characteristic of sample no.6, wavelength 850 nm **[12]**

.

2.3. Channel Models for Radio on Visible (RoVL) Communication System

The RoVL project has introduced an innovative alternative for cell phone connectivity in RF restricted or poor signal connectivity regions. This paper presents a brief theoretical study on the attributes of channel modelling, influencing mobile signal transmission in an indoor environment.

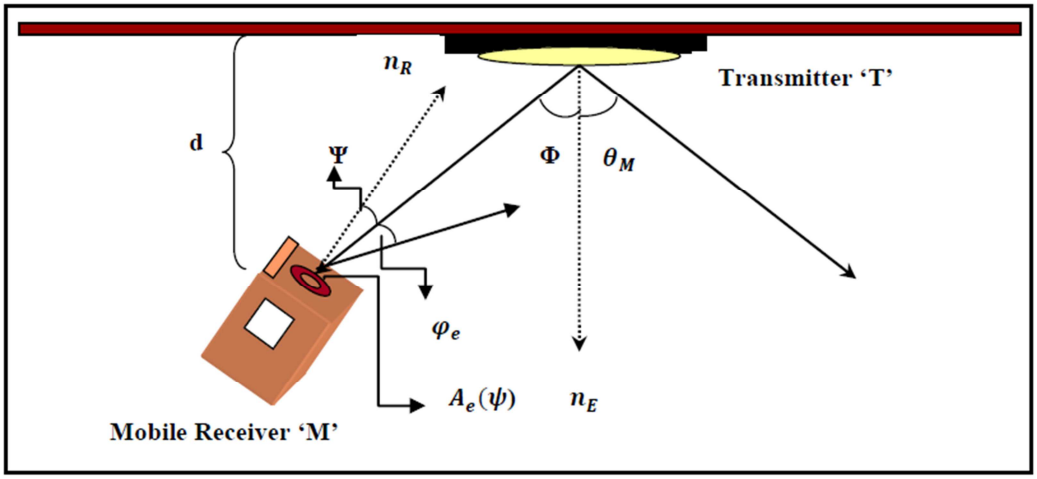

Fig.9. Directed line-of-sight (LOS) ray geometry for mobile telephony **[23]**

In the next figure is shown diffuse reflection inside a room that comes from the wall or any reflector material.

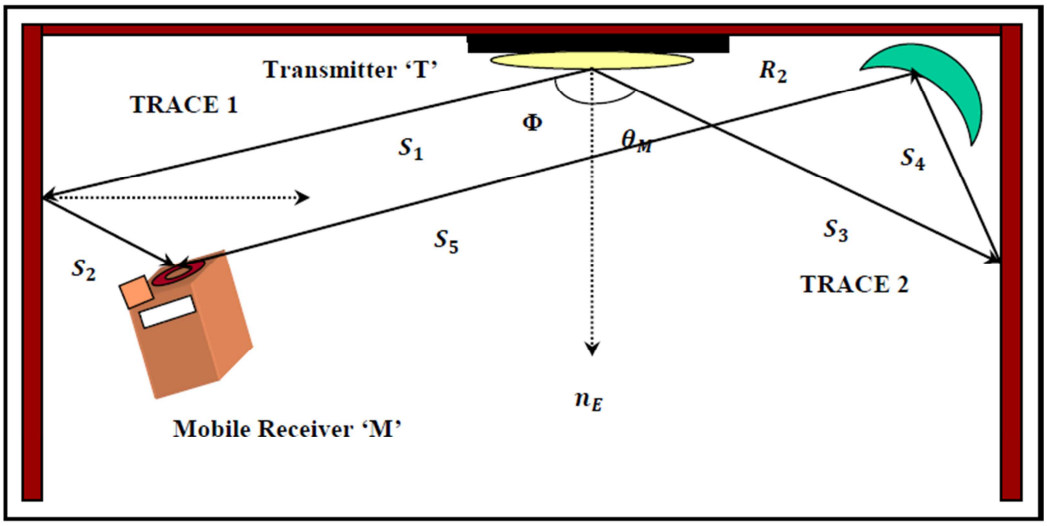

Fig.10. Diffuse ray geometry for mobile telephony through visible light **[23]**

Therefore multiple reflections scattered from surfaces, walls and furniture affect the channel model in mobile telephony. The received power of optical radiation varies depending upon the material of the scattering surface and the number of reflections as shown in fig.10.

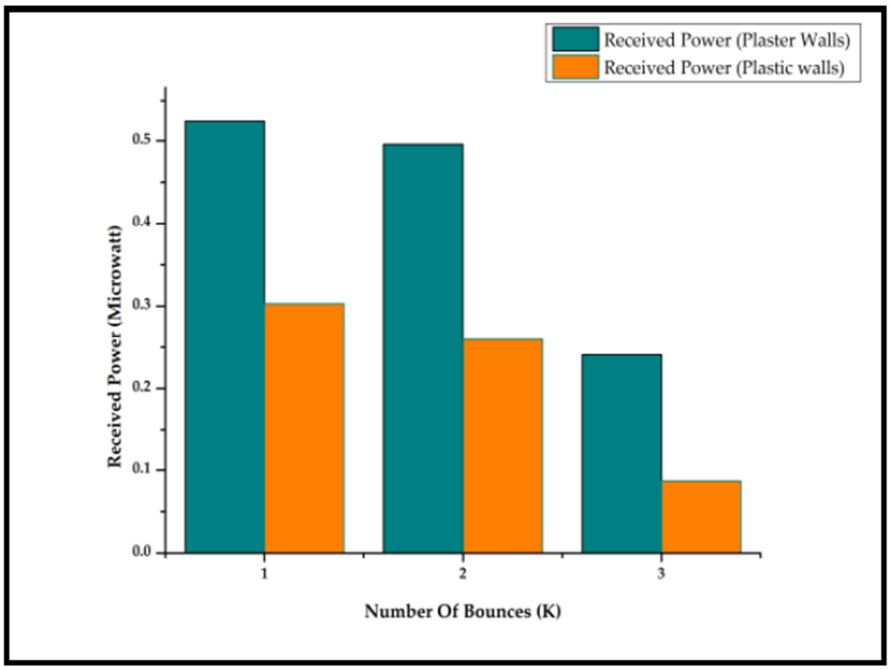

Fig.11. Received optical power for 3 bounces - Infrared case **[23]**

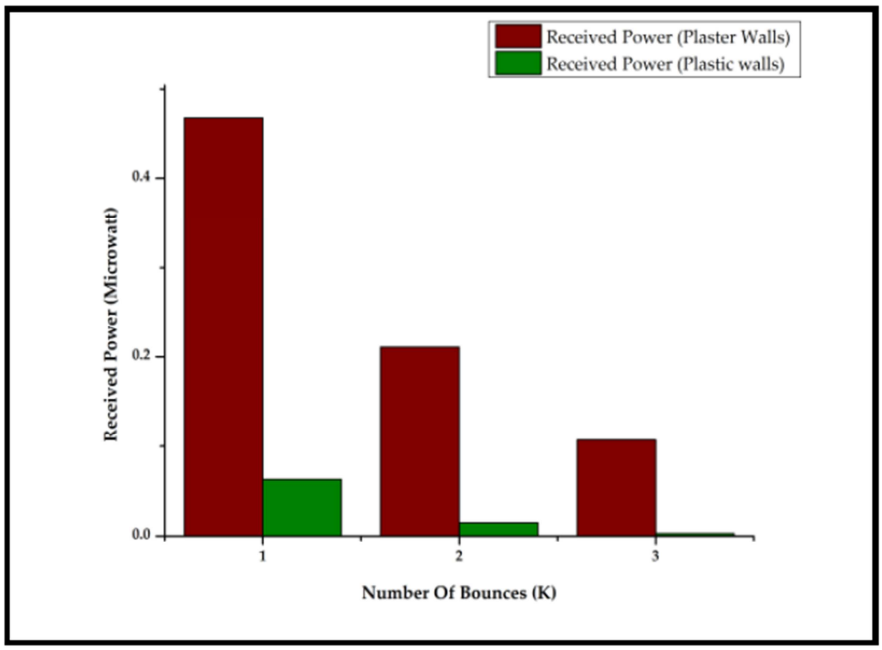

Fig.12. Received optical power for 3 bounces - Visible light case **[23]**

The received power is reduced by the reflection coefficient of the surface. It has been established by previous studies **[19]**, that the reflecting materials have greater reflectance at infrared wavelengths than in the visible light regions. It was observed that due to its high reflectance, the optical power received by the IR receivers is much greater than those of visible light receivers, as can be observed in fig. 11 and fig.12. Therefore it is preferable to operate at higher wavelengths (infrared region).

2.4. Other related projects

The other of the related papers is briefly explained in the following:

2.4.1 Model for indoor wireless optical link

In IWOL the laser beam carrying the information is propagated through the room and reflected on the walls and various objects. An IWOL works in the IR spectral region. The influence of surface reflectivity on received power is simulated by a relative directional reflectivity of surface (RDR) **[13, 14]**.

2.4.2 Simulation of reflected and scattered laser radiation

This paper presents a computer simulation of reflected and scattered laser radiation for calculating the angle of laser shields performed with Laser Shield Solver computer program. The authors describe a method of calculating the shield angle of laser shields which protect workers against reflected and scattered laser radiation and which are made from different materials **[26]**.

2.4.3 The near infrared reflective material's surfaces

The near infrared signals reflected by different surfaces are studied. The transmitted signals are reflected by different surface obstacles for varied distances among the receiver, reflector and remote controller **[17].**

3. Fundamentals

The optical communications technology is also concerned with the transmission of information with light. Light is an electromagnetic wave. The spectrum of radiation with different wavelength is shown in the table 3.

Wavelength	Designation of the radiation
< 100 nm	ionizing radiation
100 to 280 nm	UV-C
280 to 315 nm	UV-B
315 to 380 nm	UV-A
380 to 780 nm	Visible Light
780 to 1400 nm	IR-A
1,4 to 3 μm	IR-B
3 to 1000 μm	IR-C

Table 3.Designation of radiation **[1]**

In theory, the characteristics of light show that it can be treated as electromagnetic wave. Features of the optics like free space optical propagation, refraction, reflection, Gaussian beam distribution, diffuse beam distribution and optical properties of materials will be described **[1]**

3.1. Indoor Free space optical propagation

This technology becomes today a significant field for the researchers. Indoor optical wireless link describes the light source's beam propagation through the room and beam reflection on the walls or the various objects. In the figure a scheme of the experimental measuring chain arranged in the room model is shown in fig.13 **[13, 14]**.

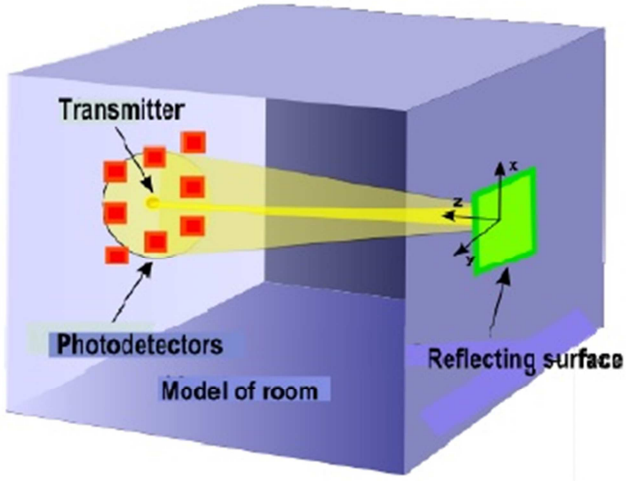

Fig.13. Basic principle of the RDR measurement **[13]**

So, in indoor FSO there are the direct beams from the optical transmitter and also the reflected beams from different material surfaces. Two optical wireless links are shown in the fig.14.

a) b)

Fig.14. Optical wireless LANs: a) diffuse link and b) line of sight **[6]**

As a medium for short-range, indoor communication, infrared radiation offers several significant advantages over radio. Infrared emitters and detectors capable of high speed operation are available at low cost. Infrared and visible light are close together in wavelength, and they exhibit qualitatively similar behavior. Both are absorbed by dark objects, diffusely reflected by light-colored objects, and directionally reflected from shiny surfaces **[18]**. The optical source converts the electrical signal to an optical signal, while inverse of source is the receiver or detector (converts optical power into electrical current). As optical sources are light emitting diodes (LEDs) or laser diodes (LDs), whereas as detectors is photodiodes (PDs). Optical sources may be divided into two groups: point sources and surface sources. LDs belong to point sources, while LEDs belong to surface sources. The beam of LDs may be approximated by a Gaussian beam. LEDs or incandescent bulbs may have approximately a Lambertian radiation pattern **[6, 35]**.

The surfaces can be a mirror (specular), diffuse or a combination of both. A special case is an absolute reflection. Variants of reflections are shown in fig.15 **[13]**.

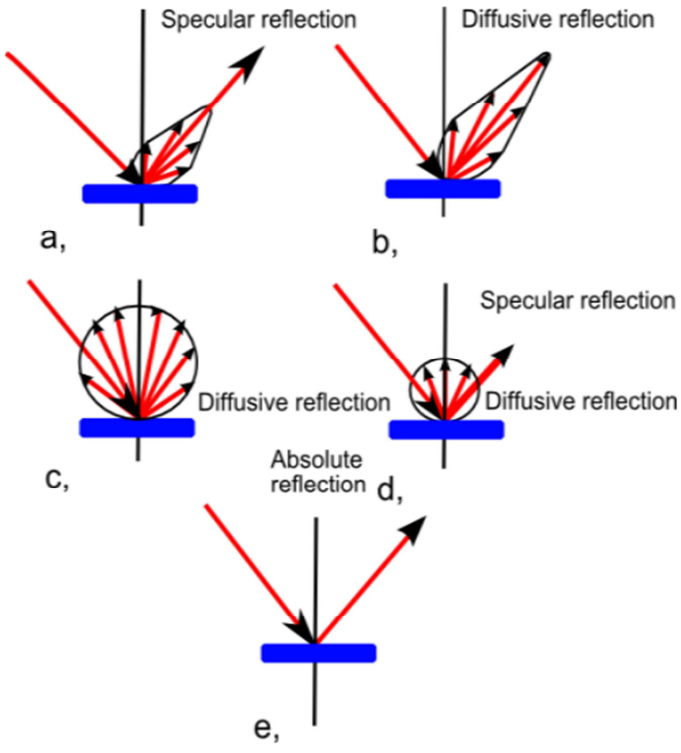

Fig.15. Types of reflection **[13]**

3.2. Reflection and refraction

In the optics special characteristics of the electromagnetic wave are used - reflection and refraction. These arise whenever the wave in differently close media spreads. The following illustration shows geometry of the propagation vectors, and of a diagonally refraction, reflected respectively refracted homogeneous plane wave.

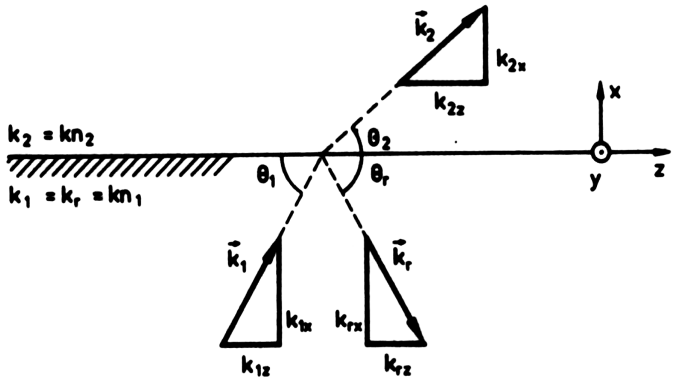

Fig.16. Geometry of the propagation vectors **[1]**

The boundary surface conditions for the tangential components of the field strengths must be fulfilled for all times and for all places. That is, that the phase lags of the regarded waves must be alike along the boundary surface.

$$\tau_{\Phi 1z} = \tau_{\Phi rz} = \tau_{\Phi 2z} \text{ or } \qquad \frac{k_{1z}}{\omega} = \frac{k_{rz}}{\omega} = \frac{k_{2z}}{\omega} \qquad \text{or} \qquad k_{1z} = k_{rz} = k_{2z}$$

From this the measure of angle of refraction Θ_2 and reflection Θ_r angles in relation to the angle of incidence Θ_1 can be determined:

$$k_1 \cos\Theta_1 = k_r \cos\Theta_r = k_2 \cos\Theta_2$$

$$n_1 \cos\Theta_1 = n_r \cos\Theta_r = n_2 \cos\Theta_2$$

By the reflection law (with $n_1 = n_r$):

$$\Theta_r = \Theta_1 \tag{1.1}$$

And refraction law:

$$n_1 \cos\Theta_1 = n_2 \cos\Theta_2 \tag{1.2}$$

(also $n_1 \sin\varphi_1 = n_2 \sin\varphi_2$ is given)

3.2.1. Reflection factors of an electrically transverse polarized wave (TE)

We assume that the incident wave comes from the optically thicker medium. Now the case of the electrically transverse polarized wave is treated ($\vec{E}_1$ stands perpendicularly on the plane of incidence and is arranged parallel to the plane boundary surface). The incident plan wave has the unchanged electrical field strength $\vec{E}_{1\perp} = E_1 \cdot \vec{e}_y$, the magnetic field strength goes only with its boundary surface-parallel component $\vec{H}_{1\perp} = H_{1z} \cdot \vec{e}_z = H_1 \sin\Theta_1 \cdot \vec{e}_z$ to the boundary surface. **[1]**

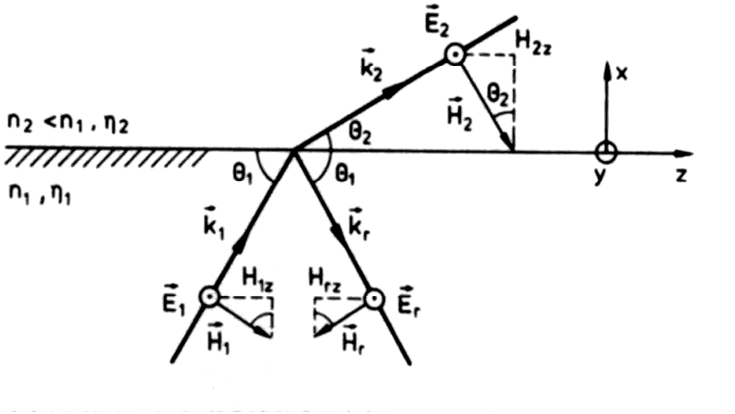

Fig.17. Reflection factor with TE polarization **[1]**

For the field wave resistance, one get

$$\eta_{1\perp} = \frac{E_1}{H_1 \sin\Theta_1} = \frac{\eta_1}{\sin\Theta_1} = \frac{\eta_0}{n_1 \sin\Theta_1}$$

The field strengths which are perpendicular to the wave occurring in second medium:

$$\vec{E}_{2\perp} = E_2 \cdot \vec{e}_y \qquad \text{and} \qquad \vec{H}_{2\perp} = H_{2z} \cdot \vec{e}_z = H_2 \sin\Theta_2 \cdot \vec{e}_z$$

The appropriate field resistance reads therefore:

$$\eta_{2\perp} = \frac{\eta_2}{\sin\Theta_2} = \frac{\eta_0}{n_2 \sin\Theta_2}$$

Thus the reflection factor can be written down with transverse electrical polarization (TE) as follows:

$$\underline{r_{TE}} = \frac{\eta_{2\perp} - \eta_{1\perp}}{\eta_{2\perp} + \eta_{1\perp}} = \frac{n_1 \sin\Theta_1 - n_2 \sin\Theta_2}{n_1 \sin\Theta_1 + n_2 \sin\Theta_2} = -\underline{r_{mTE}} \qquad (1.3)$$

$-\underline{r_{mTE}}$ ... magnetic reflection factor

If one extends the break with k, then arises also with: $k_{1x} = kn_1 \sin\Theta_1$ and $k_{2x} = kn_2 \sin\Theta_2$

$$\underline{r_{TE}} = \frac{k_{1x} - k_{2x}}{k_{1x} + k_{2x}} = r_{TE} \cdot e^{j\rho_{TE}}$$

With the help of refraction law:

$$\cos\Theta_2 = \frac{n_1}{n_2}\cos\Theta_1 \quad \text{or} \quad \sin\Theta_2 = \sqrt{1 - \left(\frac{n_1}{n_2}\cos\Theta_1\right)^2}$$

Arises also for reflection factor:

$$\underline{r_{TE}} = \frac{n_1 \sin\Theta_1 - \sqrt{n_2^2 - n_1^2 \cos^2\Theta_1}}{n_1 \sin\Theta_1 + \sqrt{n_2^2 - n_1^2 \cos^2\Theta_1}}$$

The reflection factor depends thus only on the angle of incidence and on the two refractive indices **[1].**

Under the condition $n_1 > n_2$, know the following cases are differentiated:

1. $\Theta_1 = 90°$ (perpendicular incidence): Amplitude und Phase of Reflections factor are:

$r_{TE} = \frac{n_1 - n_2}{n_1 + n_2}$ respectively. $\rho_{TE} = 0$ (real value)
A phase pure partial reflection arises.

2. $\Theta_{1c} < \Theta_1 < 90°$ (diagonal incidence): Likewise a phase pure partial reflection arises. In addition comes a regular refraction. With increasing diagonal of the incidence the reflection factor increases.

3. $\Theta_1 = \Theta_{1c}$ (critical incidence): The reflection factor $r_{TE} = 1$ and the phase $\rho_{TE} = 0$. It occurs thus a phase pure total reflection (as with an open-circuited load conduction)

4. $0 < \Theta_1 < \Theta_{1c}$ (over critical incidence): A total reflection with rapid phase change occurs. The broken wave fades away exponentially, since k_{2x} is imaginary. The reflection factor is:

$$\underline{r_{TE}} = \frac{k_{1x} + j\alpha_{2x}}{k_{1x} - j\alpha_{2x}} = 1 \cdot e^{j\rho_{TE}} \quad \text{with} \quad \rho_{TE} = 2\arctan\frac{\alpha_{2x}}{k_{1x}} = 2\arctan\frac{\sqrt{\cos^2\Theta_1 - \cos^2\Theta_{1c}}}{\sin\Theta_1}$$

This situation is comparably with a conduction with more decreasing, purely inductive terminating impedance.

5. $\Theta_1 \to 0$ (touching incidence): In this case the reflection factor is $\underline{r_{TE}} = -1$. It comes to a total reflection with rapid phase change (as with a short circuit conduction).

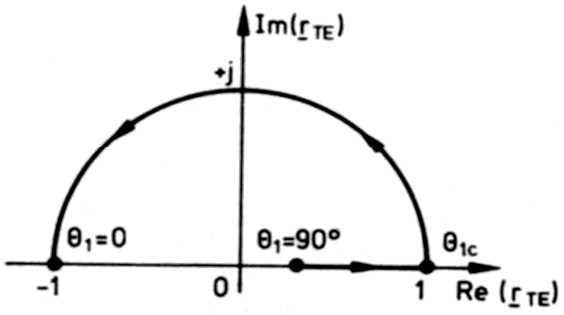

Fig.18. Electrical reflection factor with TE-polarization with incident angle **[1]**

Fig.18 shows representation of the electrical reflection factor with transverse electrical polarization of an incident homogeneous plan wave as a function of the angle Θ_1 of the incidence on a dielectric boundary surface. The incident wave comes from the optically thicker medium.

3.2.2. Reflection factors of an incident magnetically transverse polarized wave (TM)

In principle a same situation as in the previous chapter, with the difference that the magnetic field vector of the incident plan wave stands now perpendicularly on the plane of incidence (the paper plane). That is called we sets for transversal magnetic polarization ahead (index TM) **[1].**

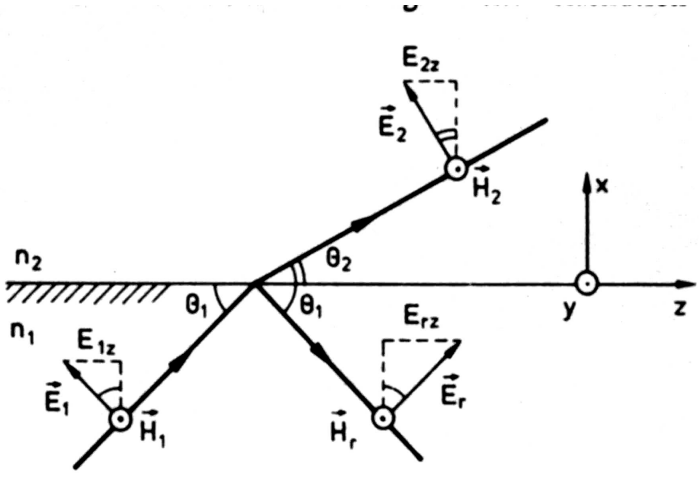

Fig.19. Reflection factor with TM polarization **[1]**

The partial plan waves have the following characteristic wave impedances in this case:

$$\eta_{1\perp} = \frac{E_{1z}}{H_1} = \frac{E_1 \sin\Theta_1}{H_1} = \eta_1 \sin\Theta_1 = \eta_0 \frac{\sin\Theta_1}{n_1}$$

$$\eta_{2\perp} = \frac{E_{2z}}{H_2} = \frac{E_2 \sin\Theta_2}{H_2} = \eta_2 \sin\Theta_2 = \eta_0 \frac{\sin\Theta_2}{n_2}$$

Thus follows for the reflection factor $\underline{r_{TM}}$ as ratio of tangential components:

$$\underline{r_{TM}} = \frac{\eta_{2\perp} - \eta_{1\perp}}{\eta_{2\perp} + \eta_{1\perp}} = \frac{n_1 \sin\Theta_2 - n_2 \sin\Theta_1}{n_1 \sin\Theta_2 + n_2 \sin\Theta_1} = \frac{n_1^2 k_{2x} - n_2^2 k_{1x}}{n_1^2 k_{2x} + n_2^2 k_{1x}} = r_{TM} \cdot e^{j\rho_{TM}} \qquad (1.4)$$

The following cases result also here in dependence of the angle of incidence:

1. $\Theta_1 = 90°$ and $\Theta_2 = 90°$ (perpendicular incidence): It occurs phase pure partial reflection. The reflection factor is:

$$r_{TM} = \frac{n_1 - n_2}{n_1 + n_2} > 0$$

2. $90° > \Theta_1 > \Theta_{1B} > \Theta_{1c}$ (diagonal incidence): With decreasing Θ_1 reflection factor becomes more smaller. In this interval it comes to a feature which is known as Brewster effect. With the case $\underline{r_{TM}} = 0$ and the angle of incidence Θ_{1B} it comes to a total transmission with that the wave is reflection-free and refracted.

For this reflection factor one receives:

$$n_2 \sin\Theta_{1B} = n_1 \sin\Theta_{2B} \qquad \text{or} \qquad \frac{\sin\Theta_{1B}}{\sin\Theta_{2B}} = \frac{n_1}{n_2}$$

According to the refraction law $\cos\Theta_{2B} = \frac{n_1}{n_2}\cos\Theta_{1B}$ and thus it follows

$$\frac{\sin\Theta_{1B}}{\sqrt{1-\left(\frac{n_1}{n_2}\right)^2\cos^2\Theta_{1B}}}=\frac{n_1}{n_2}$$

Considering the trigonometric relations

$$\sin^2\alpha=\frac{\tan^2\alpha}{1+\tan^2\alpha} \quad \text{and} \quad \cos^2\alpha=\frac{1}{1+\tan^2\alpha}$$

the relationship for the Brewster angle results

$$\left(\frac{n_1}{n_2}\right)^2=\frac{\tan^2\Theta_{1B}}{1+\tan^2\Theta_{1B}-\left(\frac{n_1}{n_2}\right)^2} \quad \text{and with this} \quad \tan\Theta_{1B}=\frac{n_1}{n_2}$$

Θ_{1B} is greater than 45 with the transition from the thicker to the thinner medium

By the Brewster effect the refracted beam is perpendicular to the direction of the virtual reflected beam. According to the refraction law (see previous page) follows:

$$\tan\Theta_{1B}\cdot\cos\Theta_{1B}=\cos\Theta_{2B} \quad \text{or} \quad \sin\Theta_{1B}=\cos\Theta_{1B} \quad \text{and with it}$$

$\Theta_{1B}+\Theta_{2B}\equiv 90°$

Through this effect, a breakdown into different polarizations (TE or TM-Waves) is possible.

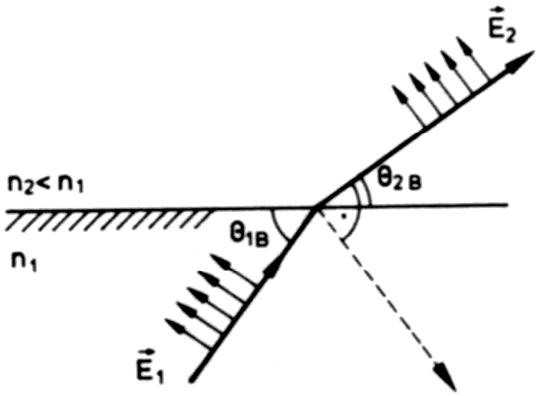

Fig.20. Interpretation of the Brewster effect **[1]**

This identity is valid for all ratios of n_1/n_2 . As an explanation of this effect it may be considered that the refracted beam, load carriers of the medium n_2 to Di-pole radiation stimulates. In vibration direction (the direction of the electric field strength = direction of the considered reflected beam) a dipole does not radiate. Therefore no reflected wave appears.

3. $\Theta_1 = \Theta_{1c}$ (Critical incidence under the boundary condition of total reflection): In this case refraction angle Θ_2 disappears, so the reflection factor becomes $\underline{r_{TM}} = -1$. Total reflection appears with phase shift of ($\rho_{TM} = 180°$).

4. $\Theta_{1c} < \Theta_1 < 0$ (Over critical incidence): Total reflection comes with phase jump. As in the previous chapter, the x-coordinate of the propagation vector in the second medium is imaginary:

With $k_{2x} = -j\alpha_{2x}$, $\alpha_{2x} > 0$ follows:

$\underline{r_{TM}} = -\dfrac{n_2^2 k_{1x} + jn_1^2 \alpha_{2x}}{n_2^2 k_{1x} - jn_1^2 \alpha_{2x}}$ therefore $\left|\underline{r_{TM}}\right| = r_{TM} = 1$ With the associated phase

$\rho_{TM} = 2\arctan\frac{n_1^2\alpha_{2x}}{n_2^2 k_{1x}} + \pi$ (The additive π derived from the negative sign)

The phase angle moves in the area $\pi \le \rho_{TM} \le 2\pi$, for the incidence angle $\Theta_{1c} \ge \Theta_1 \ge 0$. This corresponds to an electrical cable with purely capacitive impedance.

$\Theta_1 \to 0$ (touching incidence): It yields $r_{TM} = 1$ and $\rho_{TM} = 0$. It means pure phase total reflection. **[1,5]**

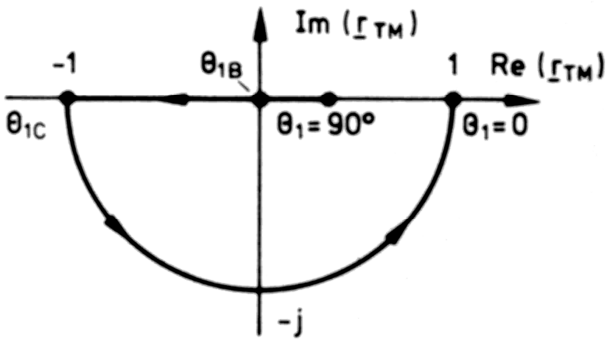

Fig.21. Electrical reflection factor with TM polarization with incident angle **[1]**

These two expressions (1.3) and (1.4), which are completely general statements applying to any linear, isotropic, homogeneous media, are known as the **Fresnel Equations [8]**. Figure plots show a reflection and transmission coefficients for incident fields with electric and magnetic polarization as a function of incident angle Θ_1 for an air-glass interface ($n_1 = 1, n_2 = 1.5$) **[5]**.

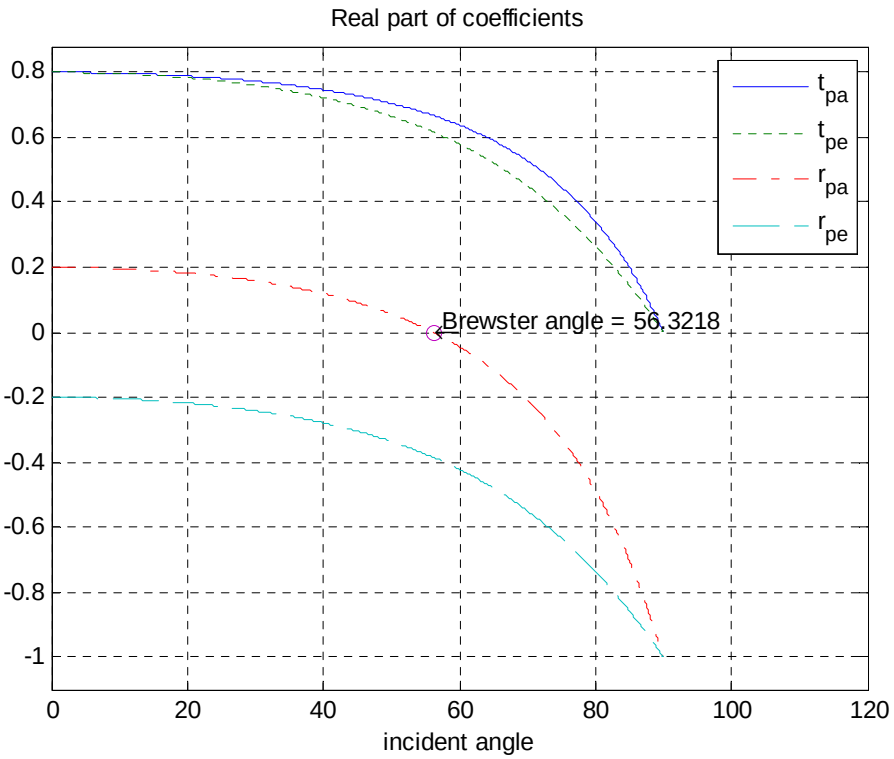

Fig.22. Reflection and transmission coefficients (real part) **[5]**

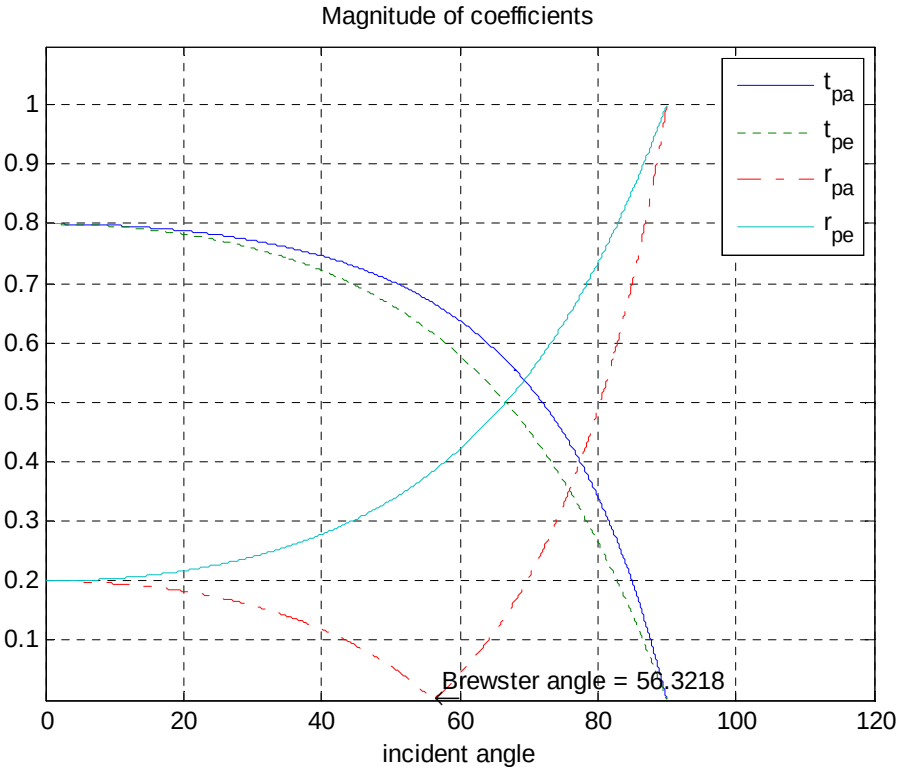

Fig.23. Magnitude of coefficients vs. incident angle **[5]**

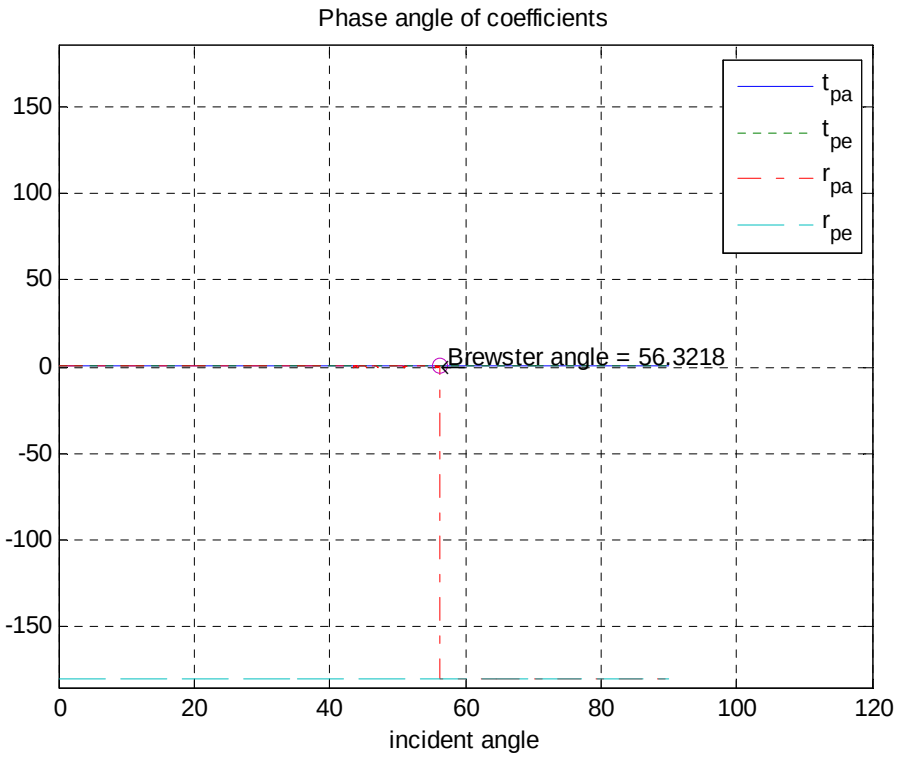

Fig.24. Phase angle of coefficients vs. incident angle **[5]**

3.2.3. Reflectance and transmittance

The incident power is $I_i \operatorname{Acos} \Theta_i$; this is the energy per unit time flowing in the incident beam and it's therefore the power arriving on surface over *A*. Similarly, $I_r \operatorname{Acos} \Theta_r$ is the power in the reflected beam and $I_t \operatorname{Acos} \Theta_t$ is the power being transmitted through *A* **[8]**. We define the **reflectance *R*** to be the ratio of the reflected power to the incident power:

$$R = \frac{I_r \operatorname{Acos} \Theta_r}{I_i \operatorname{Acos} \Theta_i} \tag{1.5}$$

We define also the **transmittance *T*** as the ratio of the transmitted to the incident power and is given by:

$$T = \frac{I_t \operatorname{Acos} \Theta_t}{I_i \operatorname{Acos} \Theta_i} \tag{1.6}$$

The common form of these equations (1.5) and (1.6) is simply:

$$R + T = 1$$

If $\theta_r = \theta_i$, then reflectance is given by:

$$R = \frac{I_r \operatorname{Acos} \theta_r}{I_i \operatorname{Acos} \theta_i} = \frac{I_r}{I_i}$$

This gives us a new equation that describes the intensity of reflected beam:

$$I_r = RI_i \tag{1.7}$$

where I_i is intensity of incident beam and R is reflectance

Most of the times, reflectance is known also as reflectivity **[8, 23]**.

3.3. Gaussian beam

Optical radiation emitted from a laser diode can be described by means of the Gaussian beam theory. It will be introduced a Gaussian beam as an approximation of a real optical source (laser diode). Under ideal conditions, the light from a laser takes the form of Gaussian beam. Using geometrical optics it is able to analyze the Gaussian intensity distribution. In the following, beam spreading and intensity are shown **[20, 21]**. Unfortunately, the output from real-life lasers is not truly Gaussian (although helium neon lasers and argon-ion lasers are a very close approximation) **[26]**.

3.3.1. Beam spreading

Now we are going to discuss some important aspects of the Gaussian beam. We require and set the origin (*z=0*) of a Gaussian beam in a position where the phase front at the origin having a radius of curvature from infinity i.e. the wave is

like a plane wave at the origin. And at the origin, the spot size of the Gaussian beam is called *beam waist* $w(0) = w_0$. Therefore the beam waist w_0 is a special case of the spot size where the radius of curvature is equal to infinity **[29].** In addition, when $R = \infty$ we have a so called the *Rayleigh length (or Rayleigh range)*:

$$z_R = \frac{\pi n w_0^2}{\lambda_0} \tag{2.1}$$

Where n is the material refractive index, λ_0 is the wavelength of the beam.

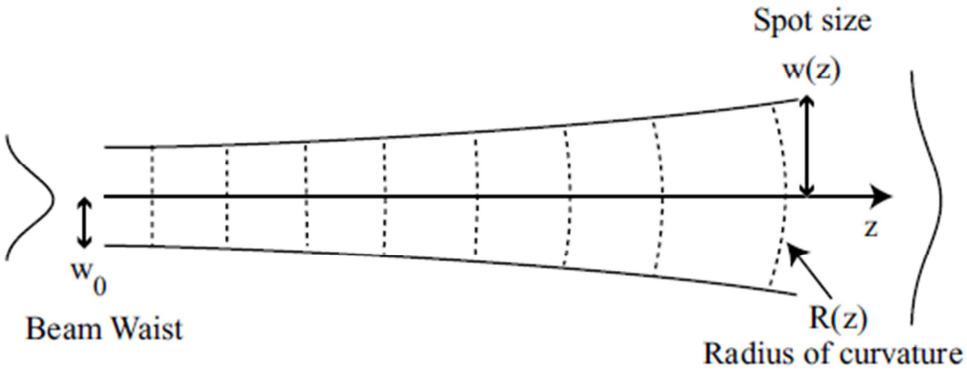

Fig.25. Beam waist radius and radius of curvature **[29]**

The spot size and wave front radius can be shown to vary with propagation distance z as

$$w^2(z) = w_0^2\left[1+\left(\frac{z}{z_R}\right)^2\right] \tag{2.2}$$

Since the relation between w and z becomes linear, a beam spreading angle can define as :

$$\frac{w(z)}{z} = \frac{w_0}{z_R} = \frac{w_0}{n\pi w_0{}^2/\lambda_0} = \frac{\lambda_0}{n\pi w_0} = \tan\theta \cong \theta$$

The beam spreading angle is:

$$\theta = \frac{\lambda_0}{n\pi w_0}$$

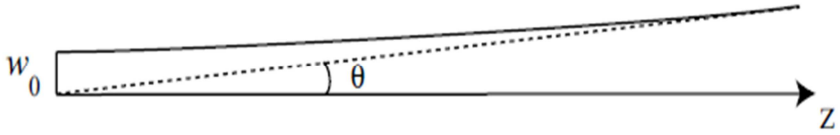

Fig.26. Beam spreading angle **[29]**

Radius of curvature is:

$$R(z) = z\left[1+\left(\frac{z_R}{z}\right)^2\right] \tag{2.3}$$

When $z = z_R$,

$$w(z) = w_0\sqrt{1+\left(\frac{z_R}{z_R}\right)^2} = \sqrt{2}w_0$$

The size of Gaussian beam has expanded by a factor of $\sqrt{2}$ as measured by a $1/e$ point of the field. Therefore z_R is a parameter that measure of how far the beam is *collimated*, and z_R is called the *Rayleigh range*. Also it is common to denote $b = 2z_R$ as the confocal parameter.

Note that the smaller the beam waist, the shorter the Rayleigh range **[2, 8, 9, 11, 28].**

3.3.2. Intensity

For a Gaussian beam the optical intensity distribution I(x,y) in the plane perpendicular to the direction of a propagation is generally elliptical and described as:

$$I(x,y,z) = I(0,0,z)e^{-2((r^2/w_x(z)^2)+(r^2/w_y(z)^2))} \tag{2.4}$$

where w_x and w_y are beam half width of Gaussian beam in x and y direction and $I(0,0,z)$ is on-axis (x=y=0) optical intensity of the beam in the distance z. Note, the central beam intensity $I(0,0,z)$ and beam half width w_x and w_y change as beam propagates in case of the divergent beam (common for optical wireless links). This change is in the far-field given by the beam divergence angle θ according to:

$$w_{x,y}(z) = z\tan(\theta_{x,y}) \tag{2.5}$$

Optical intensity is a property of the beam itself, but detected is always the optical power P integrated on a photodiode. This power P is given as:

$$P(z) = \int_s I(x,y,z)dS$$

where S – is active area of the photodiode. The total power P_{tot} transmitted by the beam is given by:

$$P_{tot}(z) = I(0,0,z)\frac{\pi}{2}w_x(z)w_y(z) \tag{2.6}$$

However, in many practical applications the transmitted beam can be approximated by the circularly symmetrical intensity distribution, where $\theta_x = \theta_y = \theta$ and also $w_x = w_y = w$ **[20]**.

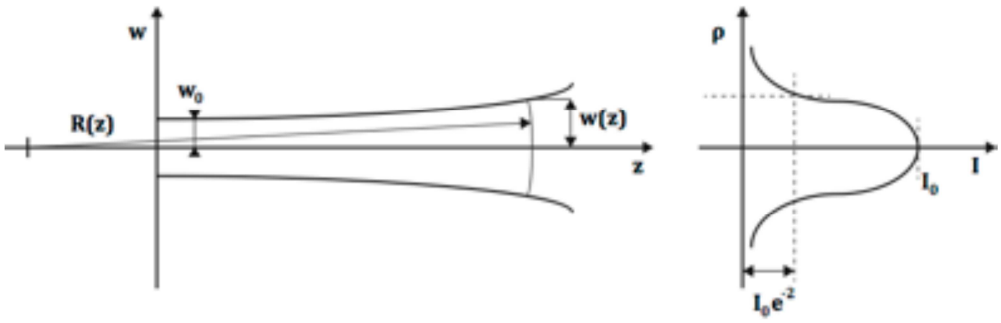

Fig.27. Gaussian beam profile **[24]**

The beam power is principally concentrated within a small cylinder surrounding the beam axis. The intensity distribution in any transverse plane is a circularly

symmetric Gaussian function centered about the beam axis **[11]**. The width of this function is minimal at the beam waist and grows gradually in both directions. The wavefronts are approximately planar near the beam waist, but they gradually curve and become approximately spherical far from the waist. The angular divergence of the wavefront normal is the minimum permitted by the wave equation for a given beam width **[2, 4, 8]**. If r=w (*beam half-width*), the beam's irradiance which depends on the square of the amplitude, is then I_0 / e^2 which is only 14% I_0. And $I = I_0 e^{-2}$, as it's supposed to, at *r=w,* where $r = \sqrt{x^2 + y^2}$ is radial distance from *z*-axis, and *z*-axis is the distance along the direction of propagation. As the beam spreads out, the curvature of the wavefronts also changes as shown in Fig.28 **[2].**

$I(w)$ - Intensity of radial distance r=w

I_0 - maximum intensity at z=0

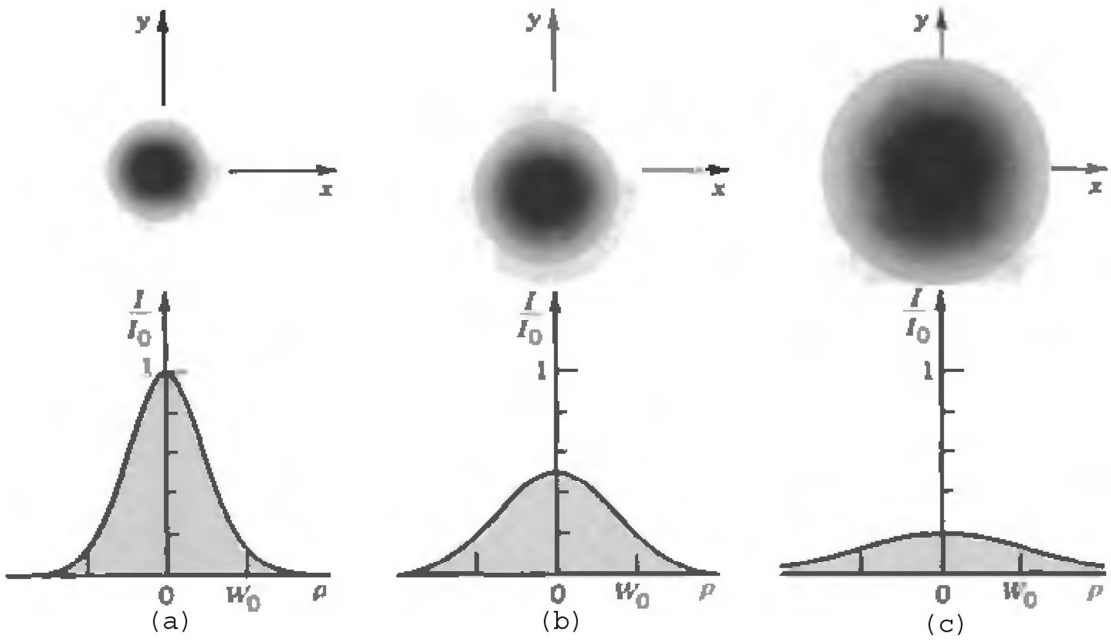

Fig.28. Intensity of Gaussian beam distribution **[2]**

3.4. Diffuse beam

There are two cases of diffuse beam distribution. One is using Gaussian beam with a help of LSD (Light Shaping Diffuser) and it distributes diffusely, and second case is using Lambertian beam distribution.

3.4.1. Gaussian beam with a Light Shaping Diffuser **(**LSD)

The irradiance distribution of fundamental Gaussian TEM_{00} laser beam at distance L is given by :

$$I(r,L) = I_0 \exp\left(\frac{-2r^2}{\mathrm{w}^2(L)}\right) = \frac{2P}{\pi w^2(L)} \exp\left(-\frac{2r^2}{w^2(L)}\right) \tag{3.1}$$

Where I_0 is the axial intensity, P is total optical power of the beam, $r^2 = x^2 + y^2$ is the position at the terminal plane, and function $\mathrm{w}(L)$ describes the evolution of the optical beam along the propagation direction L given by:

$$\mathrm{w}(L) = w_0 \left[1 + \left(\frac{\lambda L}{\pi w_0}\right)^2\right]^{0.5} \tag{3.2}$$

where λ is the wavelength of light, w_0 is the spot size radius (i.e. the radius where the field amplitude value drops to e^{-1} of the centre value) at the propagation distance L=0. From equation above we can perceive that the irradiance intensity, at a given point, is dependent only on the beam waist radius $\mathrm{w}(L)$ **[15]**.

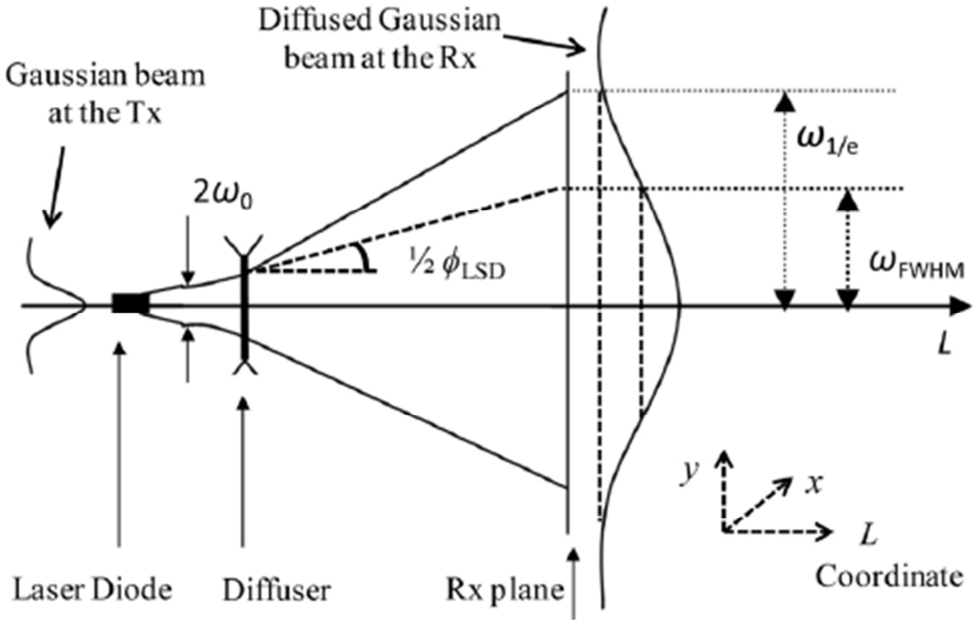

Fig.29. Gaussian beam distribution through a diffuser **[15]**

For a non-directed link covering a much wider area, the laser beam should be passed through an optical diffuser as shown in fig.29. By doing so the beam waist radius will enlarge with a diffused angle $\phi_{diff}(L)$ which is given by:

$$\phi_{diff}(L) \approx \sqrt{\phi^2{}_{div}(L) + \phi^2{}_{LSD}}$$

where $\phi_{div}(L)$ is the full width at half maximum (FWHM) divergence angle of laser diode (LD) and ϕ_{LSD} is the FWHM angle of LSD. Assuming the divergence angle of the LD is very small, i.e. $\phi_{div}(L) \ll \phi_{LSD}$, the diffused beam waist radius based on FWHM angle is given by:

$$\mathrm{w}_{FWHM}(L) = Ltan\frac{1}{2}\phi_{LSD} \tag{3.3}$$

To calculate the irradiance distribution of diffuse beam with a diffused FWHM angle, we need to convert the beam waist radius of FHWM angle to the one of full width at $1/e$ maximum angle $w_{\frac{1}{e}}(L)$.

From equation (3.1), we have:

$$I(0,L) = 2I(\mathrm{w}_{FWHM}(L), L)$$

From equation (3.3) $w_{1/e}$ is given by:

$$w_{\frac{1}{e}}(L) = \sqrt{\frac{2}{ln2}\mathrm{w}_{FWHM}(L)} \tag{3.4}$$

Therefore, for a diffused FWHM angle ϕ_{LSD} , the extended irradiance distribution of diffuse beam is given by:

$$I(r,L) = I_0 \exp\left(\frac{-\ln(2)r^2}{L^2\tan^2\left(\frac{1}{2}\phi_{LSD}\right)}\right) \tag{3.5}$$

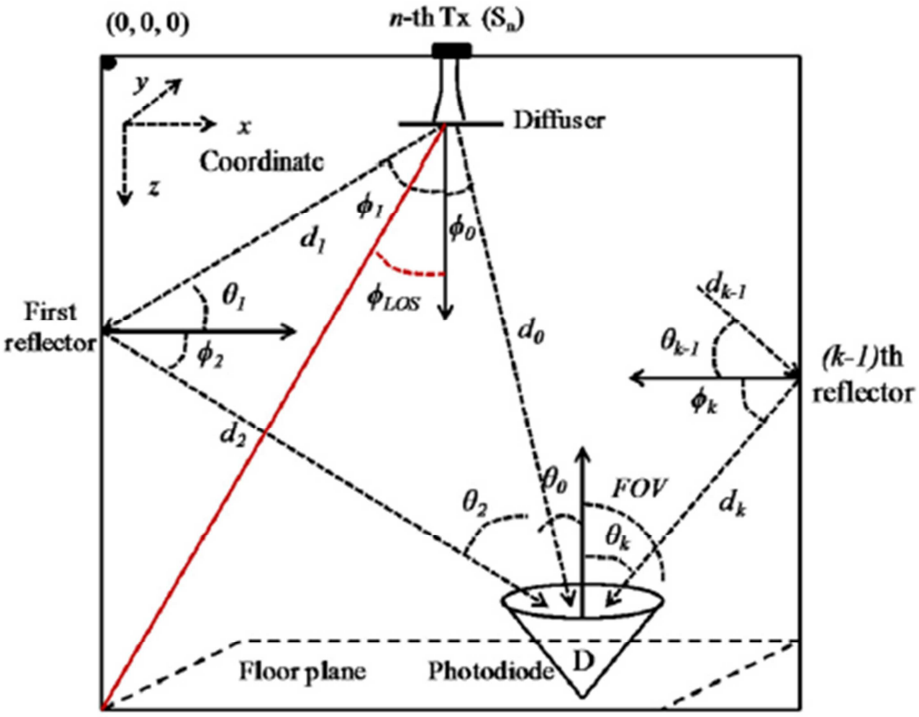

.

Fig.30. Gaussian beam distribution through a diffuser in a room **[15]**

Fig.30 illustrates a typical example of diffuse beam reflection inside the room.

3.4.2. Lambertian beam

The emitted beam of a basic LED source can be modeled as Lambertian distribution, and the radiation intensity distribution for a LOS path at the horizontal plane is given by **[3, 6, 15, 16, 18]**:

$$I(\phi) = \frac{m+1}{2\pi d^2} P cos^m(\phi) cos(\theta) \tag{3.6}$$

where m is the Lambertian order of radiation, ϕ is irradiance angle, θ is incident angle, and d is the transmission distance between source and receiver. For a given half power angle $\phi_{1/2}$, the Lambertian radiant order is:

$$m = -\frac{\ln(2)}{\ln(\cos\left(\phi_{\frac{1}{2}}\right))} \tag{3.7}$$

For example, $\phi_{1/2} = 60°$ (Lambertian transmitter) corresponds to $m = 1$, while $\phi_{1/2} = 15°$ (typical directed transmitter) corresponds to $m = 20$. A simulation program for indoor visible light communication environment based on MATLAB is presented in **[25]**. In this paper, a simulation program calculates the illumination distribution and received signal waveform considering the positions of the transmitters and the reflections on walls. It is assumed that the source of emission and the reflected points on wall have a Lambertian radiation pattern.

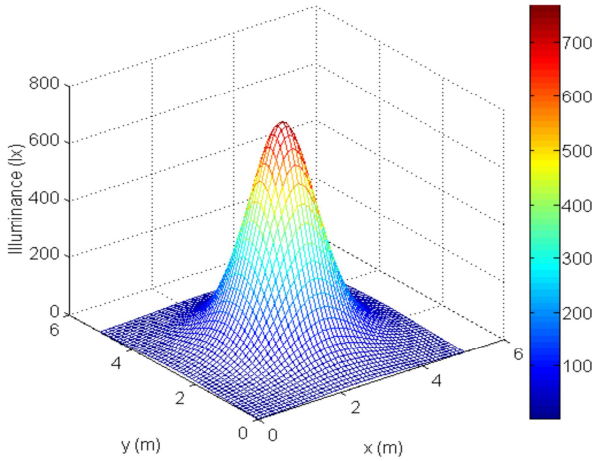

Fig.31. Distribution of illuminance in case of one transmitter **[25]**

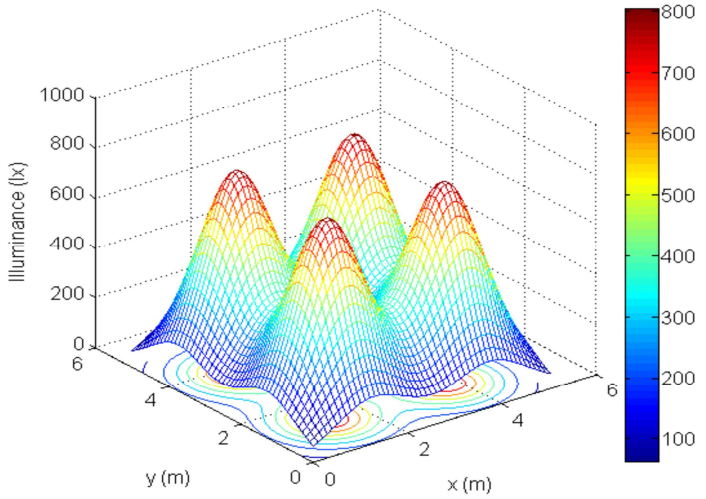

Fig.32. Illuminance distribution with 4 transmitters and semi angle of 30^{o} **[25]**

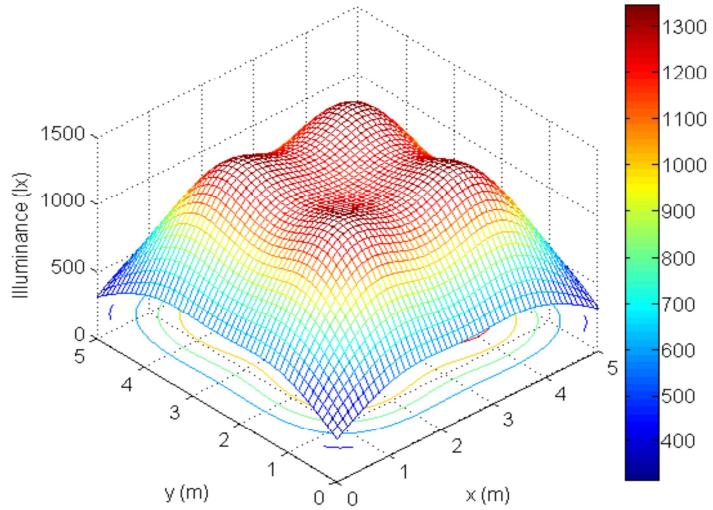

Fig.33. Illuminance distribution with 4 transmitters and semiangle of 70^{o} **[25]**

The program considers the positions of the transmitters and the reflections at each wall. For visible light communication environment, the illumination light-emitting diode is used not only as a lighting device, but also as a communication device **[25].**

3.5. Optical properties of materials

Several optical properties of materials affect the radiation beam. Some of the optical properties are: surface roughness, color, reflection coefficient, index of refraction etc. Therefor there are kinds of materials (glasses, metals, plasters, crystals etc.) with different reflectance **[3, 7].**

λ in mm	Aluminum	Silber	Gold	Copper	Platinum
300	0,923	0,176	0,377	0,336	0,576
400	0,924	0,956	0,387	0,475	0,663
500	0,918	0,979	0,477	0,6	0,714
600	0,911	0,986	0,919	0,933	0,752
700	0,897	0,989	0,97	0,975	0,772
800	0,867	0,992	0,98	0,981	0,785
900	0,891	0,993	0,984	0,984	0,805
1000	0,94	0,994	0,986	0,985	0,807
5000	0,984	0,995	0,994	0,964	0,949
10000	0,987	0,995	0,994	0,989	0,962

Table.4. Reflectance of the mirror metals **[3]**

For mirror reflection, glasses materials are used. A wide variety of common building materials are efficient diffuse infrared reflectors. In the 800–900-nm range, typical plaster walls and acoustical ceiling tiles have diffuse reflectivities in the range of 0.6–0.9, while darker materials often exhibit lower values of ρ **[18].** Most of materials (with the notable exception of glass) are approximately Lambertian reflectors i.e., they scatter light with a power per unit solid angle proportional to the cosine of the angle with respect to the surface normal, independent of the angle of incidence **[17, 33].** Lambert cosine law is defined as:

$$I = I_0 \cos(\theta) \tag{3.7}$$

where:

I - Intensity of light scattered from a point on a reflecting surface

I_0 - Incident light intensity at the maximum

θ - angle of the scattered light.

4. Reflection-Analysis on Types of Light-Beams using MATLAB®

MATLAB® provides tools to acquire, analyze, and visualize data. It also enable to document and to share your results through plots and reports or as published MATLAB code **[34]**. This chapter consists of two parts: simulation of Gaussian beam distribution and simulation of diffuse beam distribution. First part shows the case when reflective object surface is specular (mirror) with different reflection coefficients. We analyze also the Gaussian beam distribution from reflected side, when the incidence angle varies. Second part indicates the diffuse beam distribution. Taking in consider an optical source as Gaussian beam that propagates in the air, hits the object surface and reflects to a receiver as diffuse beam. Another simulation's example is when the source has a Lambertian beam in order to analyze the beam intensity in function of the irradiance angle.

4.1. Simulation of Gaussian beam distribution and mirror surface

In this simulation part are investigated:

- The reflected irradiance distribution (single and multiple reflections beam) including the reflectivity
- The reflected beam distribution when the optical source rotates with a certain angle
- The circular beam distribution transforming in an elliptical beam

For this simulation part, the parameters are given in table 5.

Specifications and constants	Symbol
Full divergence angle	Θ = 20˚
Wavelength	λ = 850nm
Distance	z = 15mm
Total power of a source	P_tot = 6mW

Table.5. Specifications for simulation of the optical beam

4.1.1. Direct beam with single and multiple reflections

First, there is the optical source that propagates the light beam direct on the mirror object's surface and it reflects back to the source's side. Incident and reflected beam distribution are analyzed.

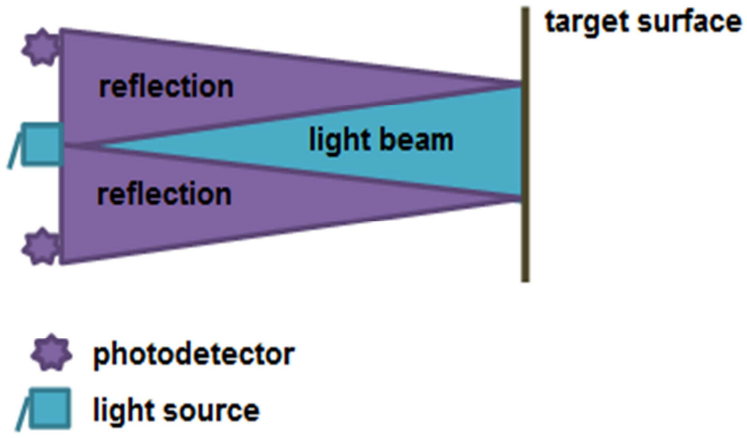

Fig.34. Gaussian beam distribution and reflection from mirror surface.

For the simulation, the equations (2.4) and (2.5) of Gaussian beam distribution are used. Fig.34. illustrates an optical beam from source to the material surface and reflected beam to the photodetector. In fig.35 the Gaussian beam has a narrow beam compare to the reflected beam. It is also evident that the intensity of reflected beam is lower compare to the incident beam. The intensity of Gaussian beam is 546 W/m^2, whereas for reflected beam it is 136.5 W/m^2.

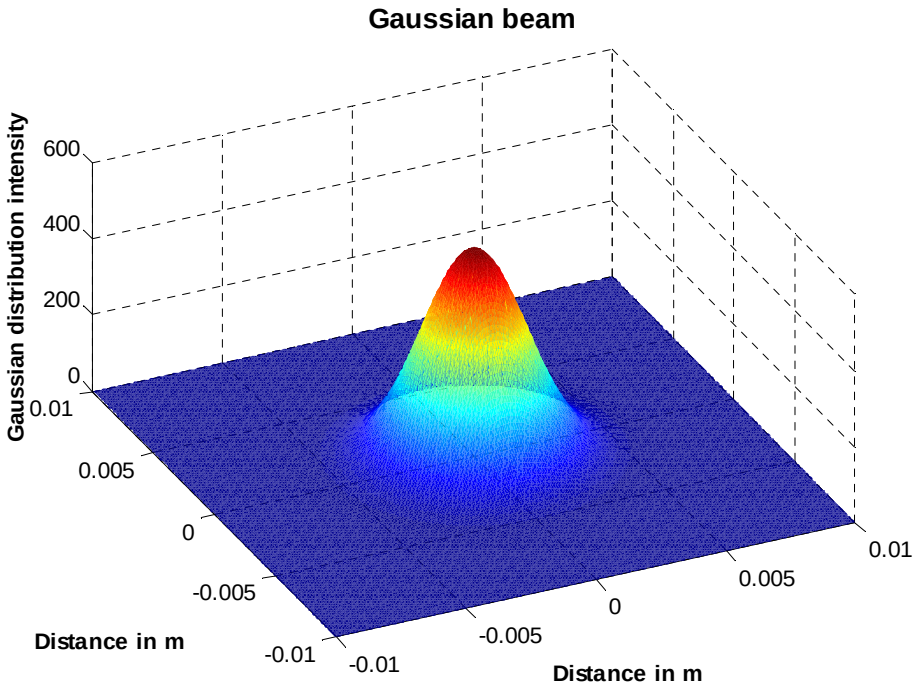

Fig.35.Gaussian beam distribution

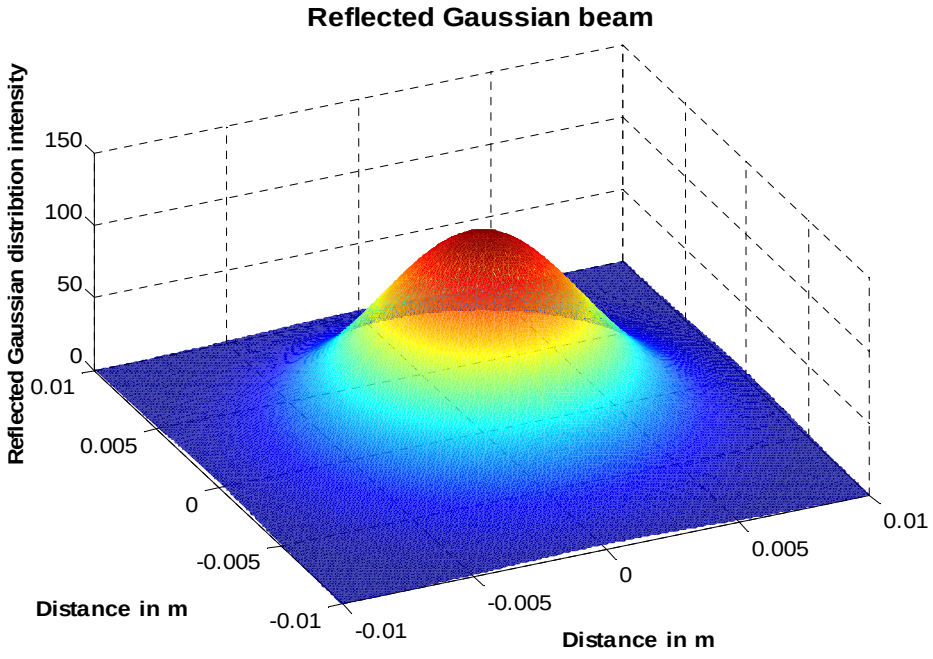

Fig.36.Reflected Gaussian beam distribution

In case of multiple reflections beam (the beam continually reflects multiple times), the Gaussian beam gets wider. As result of the multiple reflections beam, the intensity reduces.

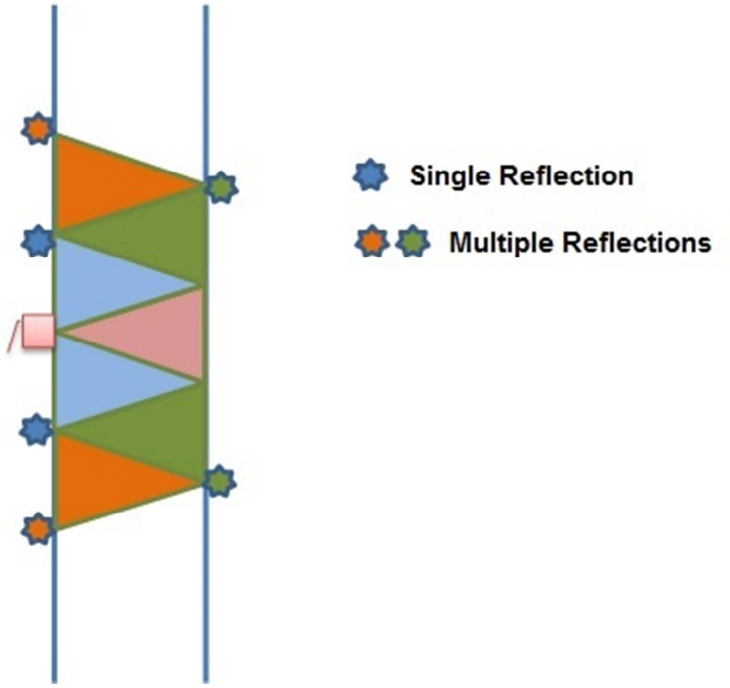

Fig.37. An illustration of multiple reflections

Fig.37 gives an illustration of multiple reflections beam. The purple color indicates the directed light beam, whereas the green indicates the same beam that reflects two times and the orange one reflects three times. From the simulation results, the intensities of second and third cases of reflection beam are 60.67 W/m^2 and 34.12 W/m^2.

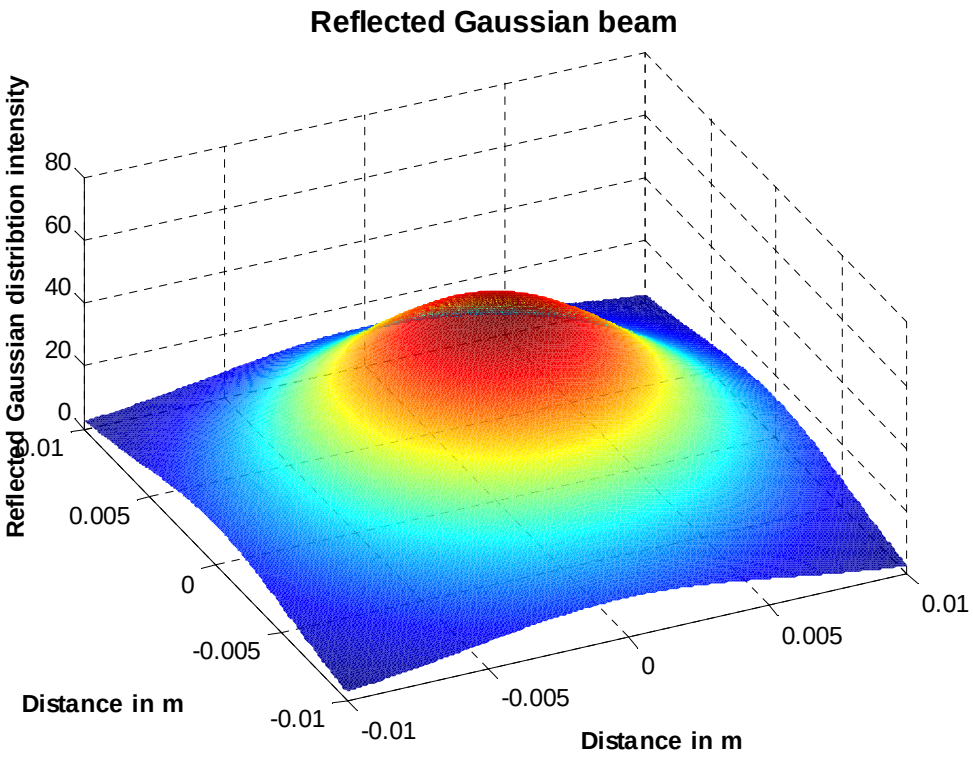

Fig.38. Intensity distribution after second reflection (green)

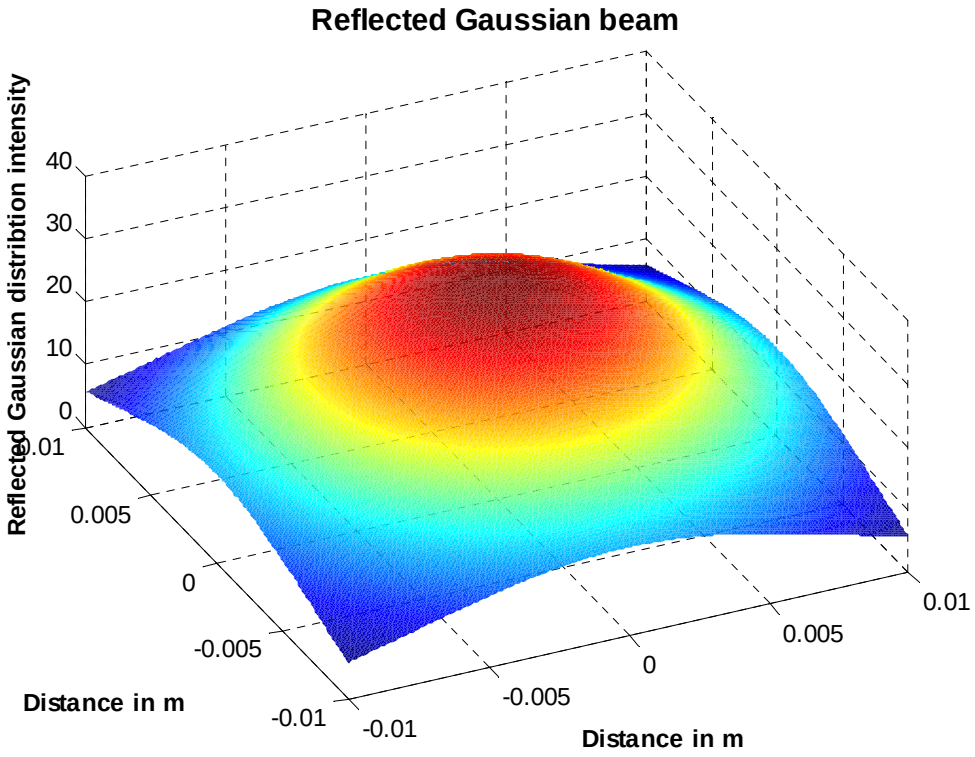

Fig.39. Intensity distribution after third reflection (orange)

4.1.2. Reflected beam and incident angle

We focus deeper in geometrical aspect for an explanation. Changing the incident angle φ affects the distance from an optical source to the surface and also, the beam is not symmetrical anymore as it illustrates in fig.37. The new distance z_1 is expressed by:

$$z_1 = \frac{z}{\cos(\varphi)}$$

where the incident angle varies $\varphi \backsim (-90^{\circ}\ to\ 90^{\circ})$.

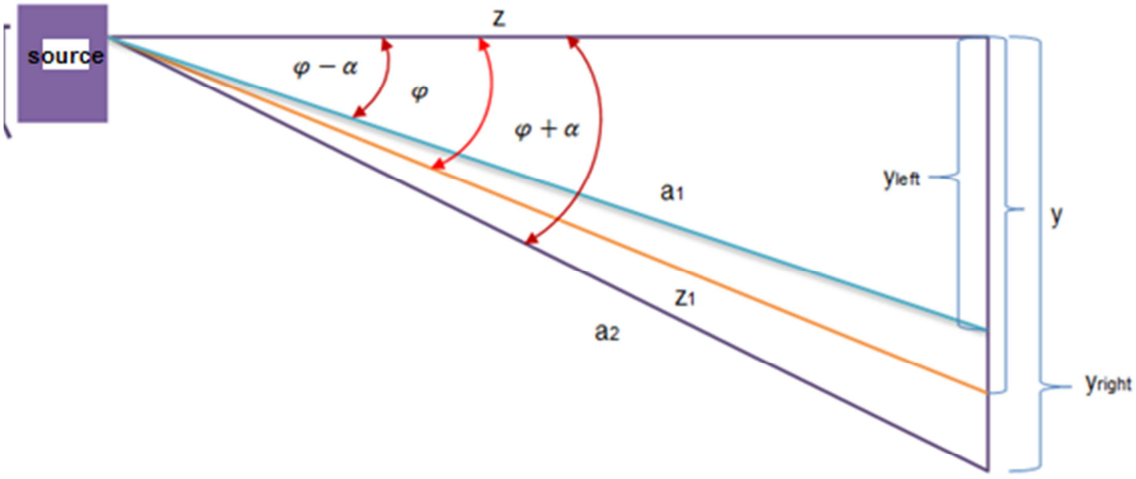

Fig.40. An illustration of light beam with an incident angle φ

We know how to calculate the beam radius with right triangle, but, now we try to find the unsymmetrical beam in a mathematical form. The beam radius with an angle at full width at half maximum $\Theta = 20^{\circ}$ and an incident angle φ is expressed by:

$$y = z\tan(\varphi)$$

In order to find the distance where the beam hits the object's surface, we separate y beam radius into two parts.

$$y_{left} = z\tan(\varphi - \alpha)$$
$$y_{right} = z\tan(\varphi + \alpha)$$

where α is the half of the Θ is 10.

A right triangle is triangle with an angle of 90 degrees (π/2 radians). The sides a, b, and c of such a triangle satisfy the Pythagorean Theorem **[31]**.

$$\boxed{a^2 = b^2 + c^2}$$

In fig.37 two distances are given:

$$a_1 = \sqrt{z^2 + {y_{left}}^2}$$
$$a_2 = \sqrt{z^2 + {y_{right}}^2}$$

Now, to express the beam radius of unsymmetrical beam, we get a vector of distances from the minimal distance z_{2min} and the maximal distance z_{2max}:

$$z_{2min} = a_1 * \cos(\alpha)$$

$$z_{2max} = a_2 * \cos(\alpha)$$

The distance vector:

$$z_2 = (z_{2min} \ldots z_{2max})$$….vector

Then we get the beam width radius w_2 as a vector from distance vector z_2.

$$w_2 = z_2\tan(\alpha)$$

Expression of the beam radius *w* with z-distance and α – semi angle at a half maximum is:

$$w = z\tan(\alpha)$$

Whereas the beam radius w_1 is given:

$$w_1 = z_1 \tan(\alpha)$$

In this situation the equations with the same parameters are used. The distance of the reflected beam is the two times of the incident beam's distance, for example if the beam travels to the target in distance from *z=15mm*, the reflected beam back to source side is *z=30mm*.

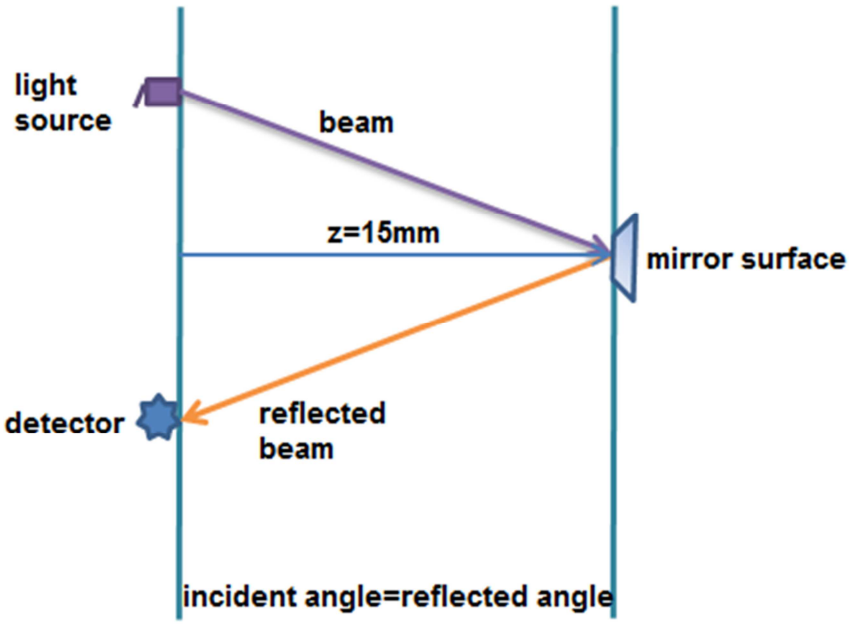

Fig.41. Illustration of reflection with an incident angle φ

Now, the Matlab plots show beam distribution with various values of incident angle φ. Where the black line is Gaussian beam on the surface and blue line is reflected beam back to the source side. Intensity of reflected beam starts to decrease on dependence of the incident angle see figures below. Fig.42, fig.43, and fig.44 indicate beam in function of incident angle. It is the same situation when the light beam propagates continually and reflects multiple times. Fig.45 shows multiple beam reflections (green line – for two bounces and red one – for three bounces).

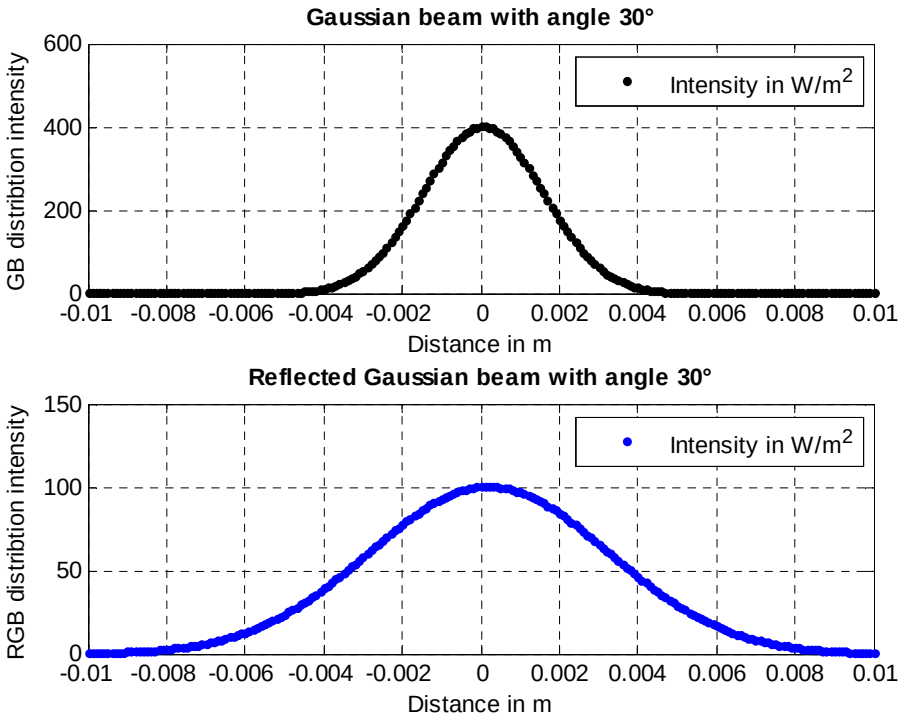

Fig.42.Gaussian beam distribution with an incident angle 30^{o}

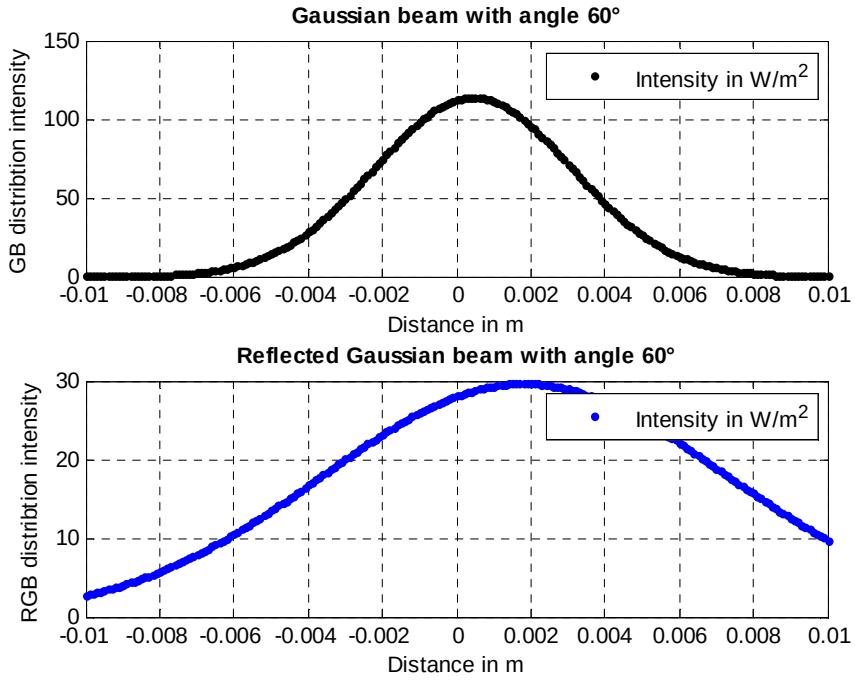

Fig.43.Gaussian beam distribution with an incident angle 60^{o}

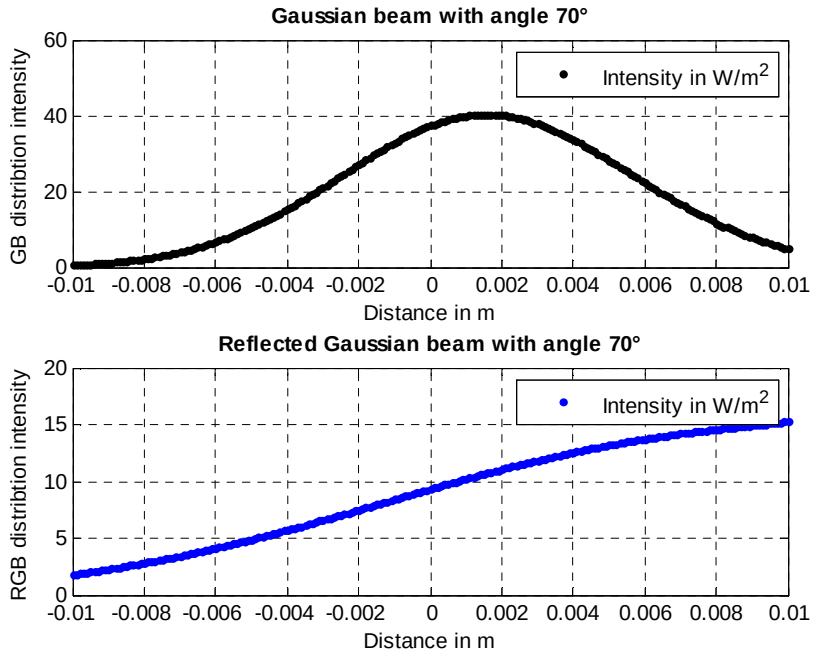

Fig.44.Gaussian beam distribution with an incident angle 70^{o}

As shown in figures the higher incident angle the lower intensity.

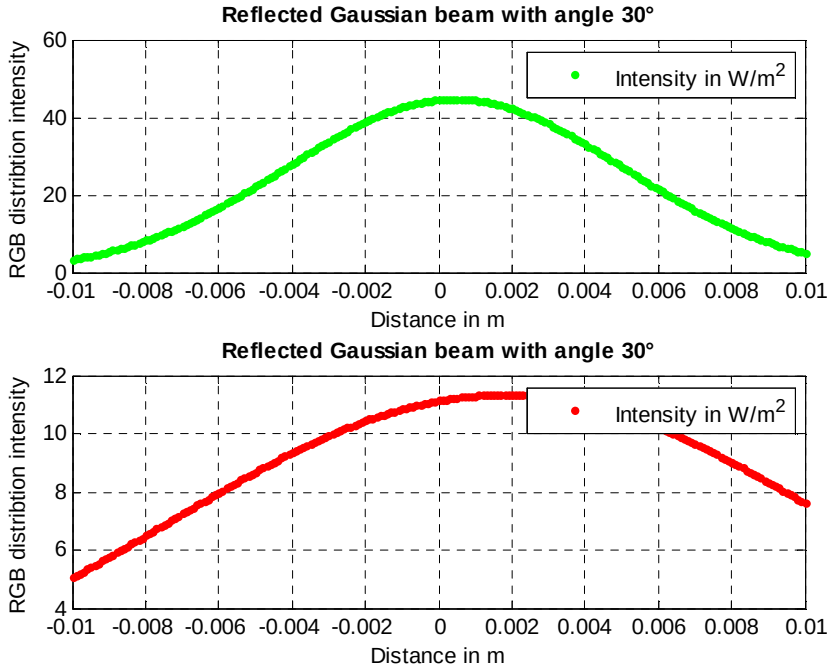

Fig.45. RGB distribution with an incident angle 30^{o} and multiple reflections

4.1.3. Direct reflected beam and reflection coefficient

As it described before in chapter 2, there are several optical properties that affect the radiation beam. Adding the reflectivity of various object surfaces on the light beam, will affect immediately the irradiance intensity.

Specifications and constants	**Symbol**
Full divergence angle	Θ = 20˚
Wavelength	λ = 850nm
Distance	z = 15mm
Total power of LD source	P_tot = 6mW
Reflectivity (reflection coefficients)	r_o = (0.2, 0.4, 0.6, 0.8, 1)

Table.6. Specifications for simulation of the optical beam adding reflectivity r_o

From equation (1.7), depending on different values of reflectivity, the intensity of reflected beam is varied. The lower reflectivity, also the intensity of reflected beam decreases.

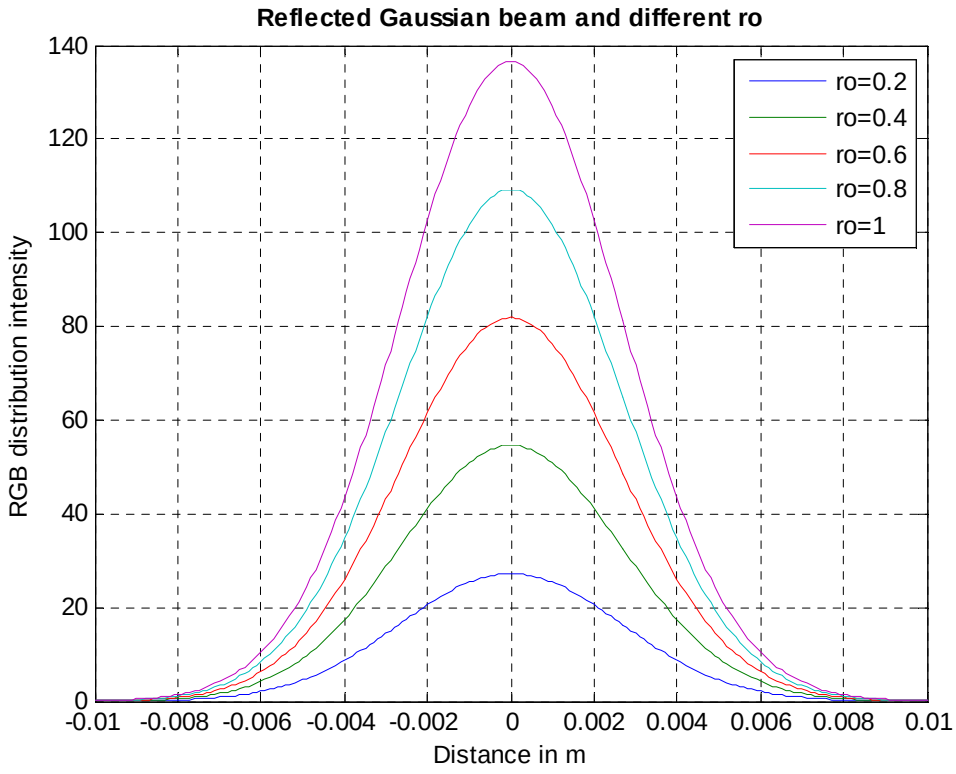

Fig.46. Gaussian beam with reflectivity (r_o=0.2, 0.4, 0.6, 0.8, 1)

4.1.4. Reflected beam and beam width angles in x and y direction

From previous chapter, the equation (2.4) for intensity of Guassian beam distribution is described as:

$$I(x,y,z) = I(0,0,z)e^{-2((r^2/w_x(z)^2)+(r^2/w_y(z)^2))}$$

$I(0,0,z)$ - intensity of the beam in direction z.

r – radial distance

And equation (2.5) of the beam waist radius in direction x and y is:

$$w_{x,y}(z) = z\tan(\theta_{x,y})$$

$\theta_{x,y}$ - beam waist angle in direction x and y.

If $\theta_x = \theta_y$, the beam waist radius has circular form as shown in fig.47.

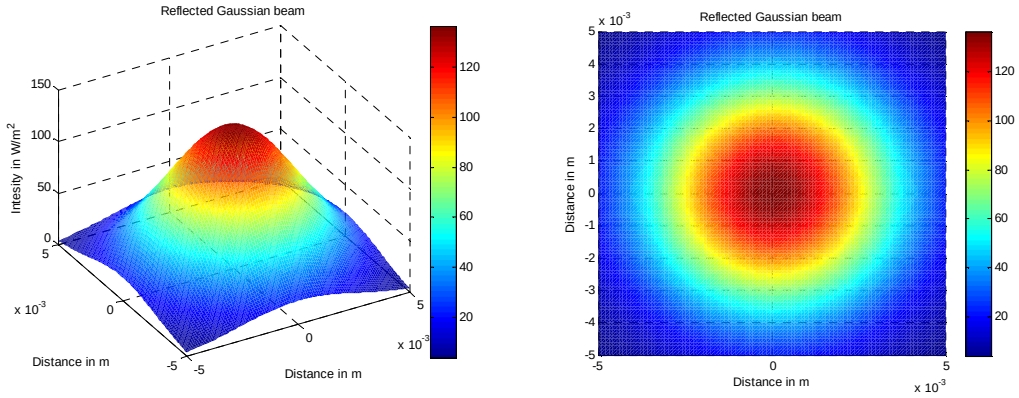

Fig.47. Circular form of reflected Gaussian beam distribution ($\theta_x = \theta_y$)

If $\theta_x \neq \theta_y$, the beam waist radius has elliptical form as shown in fig.48.

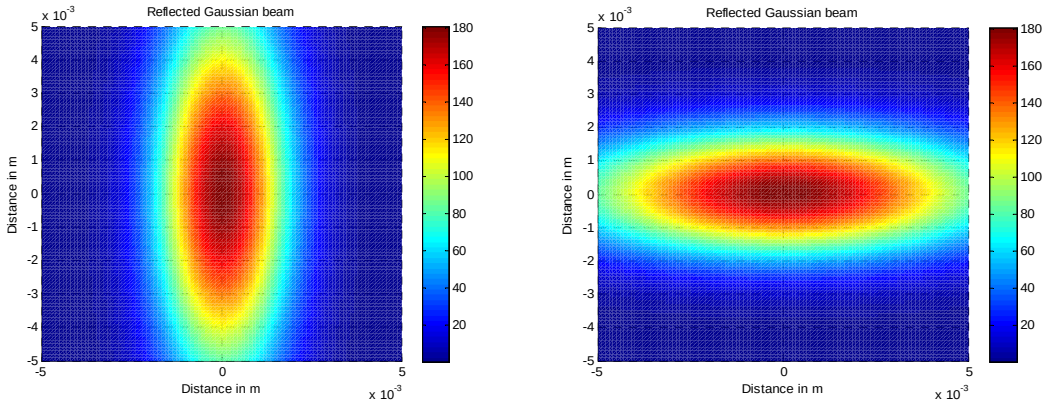

a) b)

Fig.48 Elliptical reflected beam when a) $\theta_x = 15°$, $\theta_y = 5°$ and b) $\theta_x = 5°$, $\theta_y = 15°$

4.2. Simulation of diffuse beam distribution

This is the situation when the material surface has diffuse reflection. From equations (3.4) and (3.5), the diffuse reflected beam distribution is described as:

$$I(r, 2L) = I_0 \exp\left(\frac{-2r^2}{w_{\frac{1}{e}}(2L)^2}\right)$$

The reflected diffuse beam waist radius of full width at 1/e maximum angle is:

$$w_{\frac{1}{e}}(2L) = \sqrt{2/ln(2)}\, w_{FWHM}(2L)$$

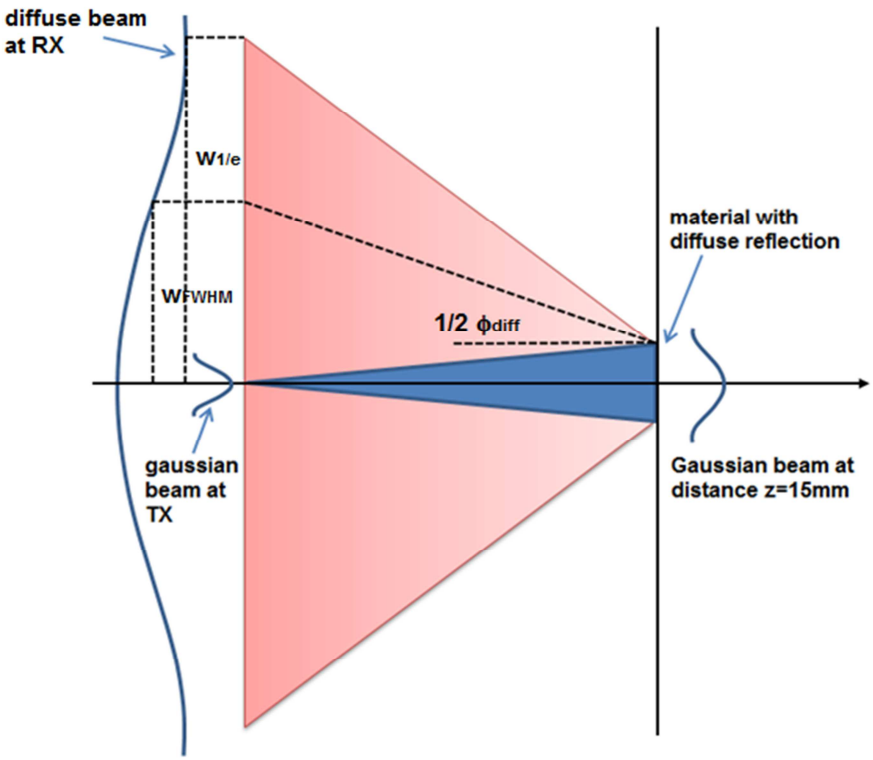

Fig.49. An illustration of diffuse beam distribution

4.2.1. Comparison of the beam waist radii

As mentioned before, from the equations, the beam width radius differs whether the surface is specular or diffuse. Fig.50 shows the comparison of the beam width radius. In the following table beam radii in function of distance are compared. It is evident from fig.50 and from table.7 the diffuse beam radius (*w_diffuse*) is wider compared to the two other beam radii - the linear and Gaussian beam radii (*w_normal* and *w_gaussian*).

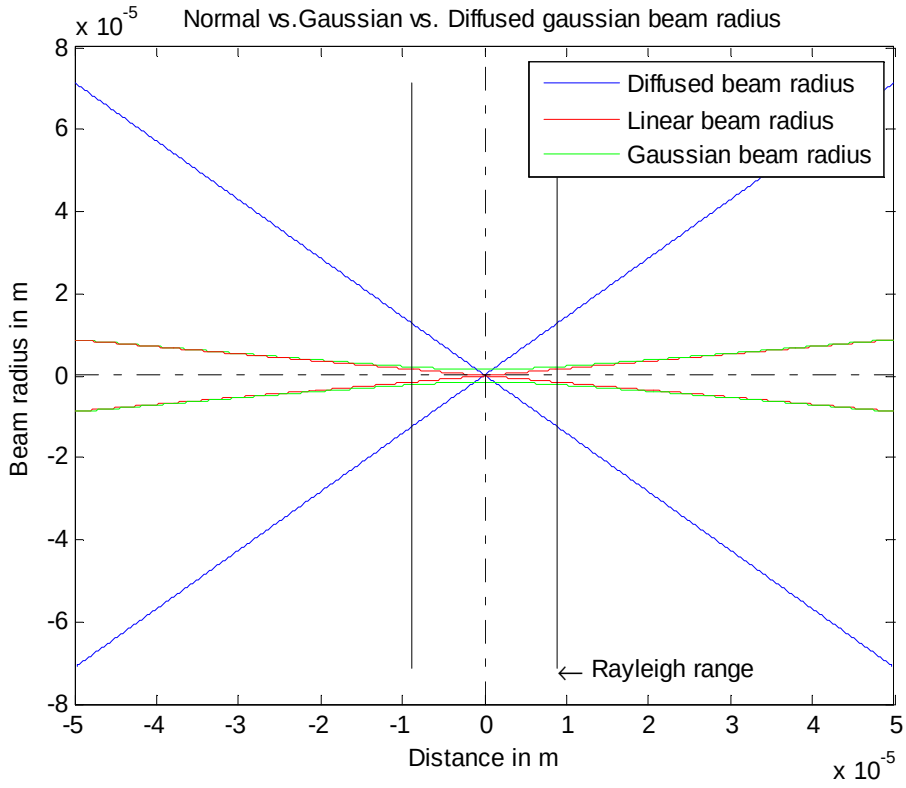

Fig.50. Comparison of the beam waist radii

Because of similarity between linear and Gaussian radius values, we assume the radius to be approximately equal.

	Distance z in mm				
	0	**1**	**2**	**3**	**4**
w_normal	***0***	***0,176***	***0,35***	***0,52***	***0,7***
w_gaussian	***0,017***	***0,17***	***0,35***	***0,52***	***0,69***
w_diffuse	***0***	***1,4***	***2,9***	***4,3***	***5,7***

Table.7. Beam width radii in function of distances (in mm)

4.2.2. Simulation of relative directional reflectivity (RDR)

The surface reflectivity includes both diffusive and specular components and the directional properties of the surface reflectivity are characterized by the RDR **[13, 14]**. The RDR is given by the equation:

$$\mathrm{RDR} = A_n \left(\frac{1+\cos(\gamma)}{2}\right)^n$$

where An is measure coefficient of the dispersed power on surface, n is measure coefficient of the directional characteristics of dispersed power on surface. Note that if n=1, then it is ideal Lambertian surface with unit reflectance, RDR = 1; If n changes and An is fix, for example n=1, 5, 10 and An = 1(scattering angle is $\gamma = 0$), then we can simulate the RDR in function of angle.

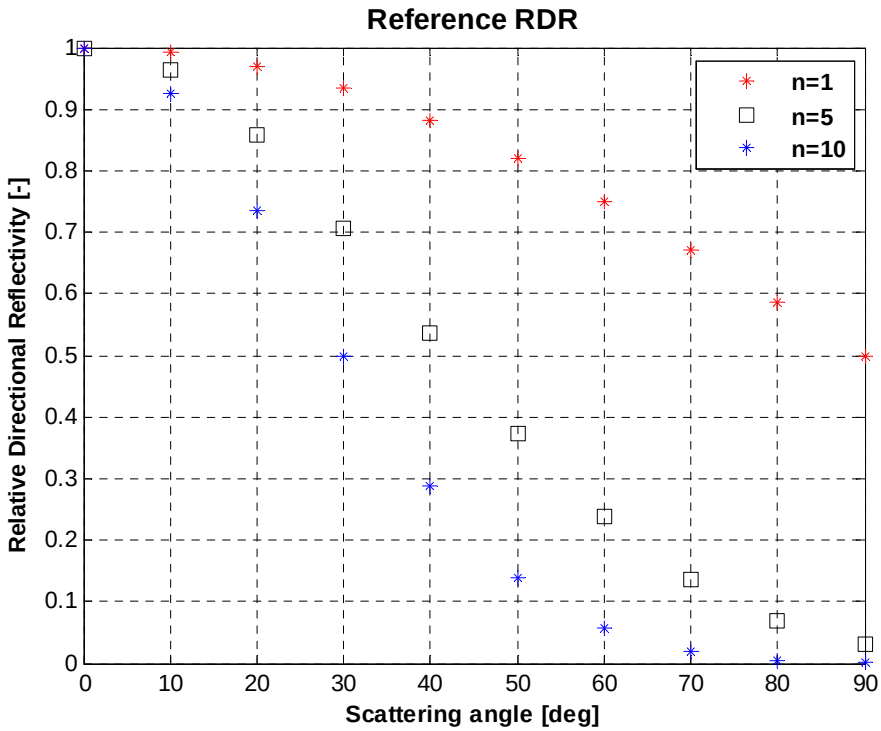

Fig.51. RDR in function of scattering angle

Fig.51 shows that in case of full diffusive surface the coefficient of directivity n is smaller.

4.2.3. Reflected diffuse beam distribution and scattering angle

For diffuse beam distribution, the beam width radius of full width at half maximum (FWHM) divergence angle of the optical source has to be smaller than the one of full width at maximum angle ($\phi_{ref}(L) = 60°, 120°$). Considering this, the intensity of reflected diffuse beam distribution presents very low values depending on scattering angle for short distance as shown in fig.52 and fig.53.

Specifications and constants	**Symbol**
Full divergence angle	Θ = 20˚
Wavelength	λ = 850nm
Distance	z = 15mm
Total power of a source	P_tot = 6mW
Reflected full width angle	ϕ = 60˚ , 120˚

Table.8. Specifications for reflected diffuse beam distribution

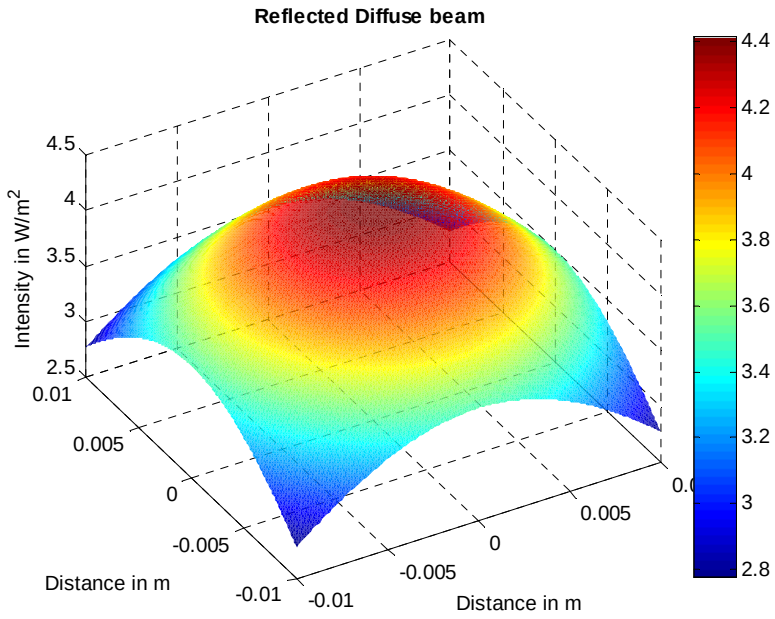

Fig.52. Reflected diffuse beam distribution *(ϕ=60^o)*

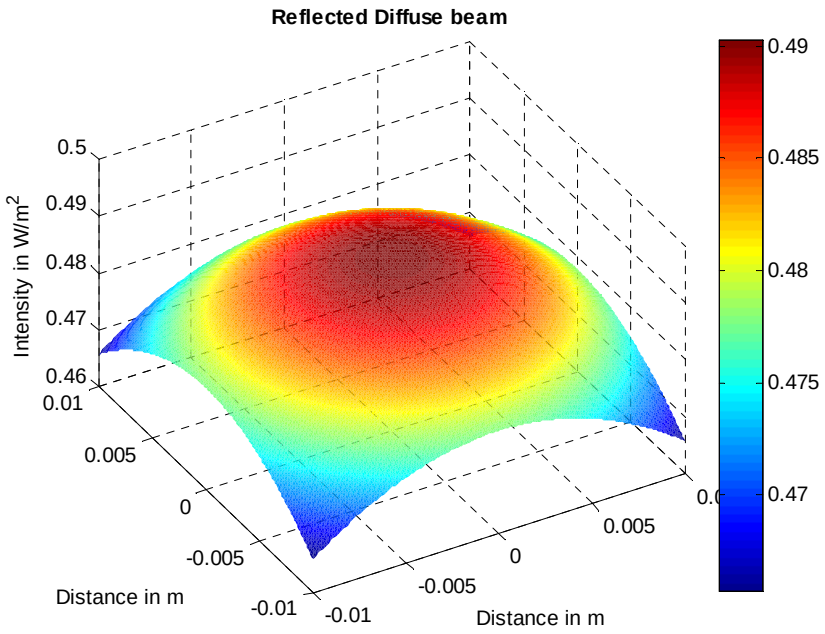

Fig.53. Reflected diffuse beam distribution ($\phi=120^{o}$)

4.2.4. Reflected diffuse beam distribution and reflection coefficient

Reflectivity affects the intensity of reflected beam. If reflectivity is 100% or $r_o=1$, the maximal value of intensity is achieved. While for small value of reflectivity, the intensity achieves minimal value. Fig.54 shows the influence of reflectivity in the reflected diffuse beam.

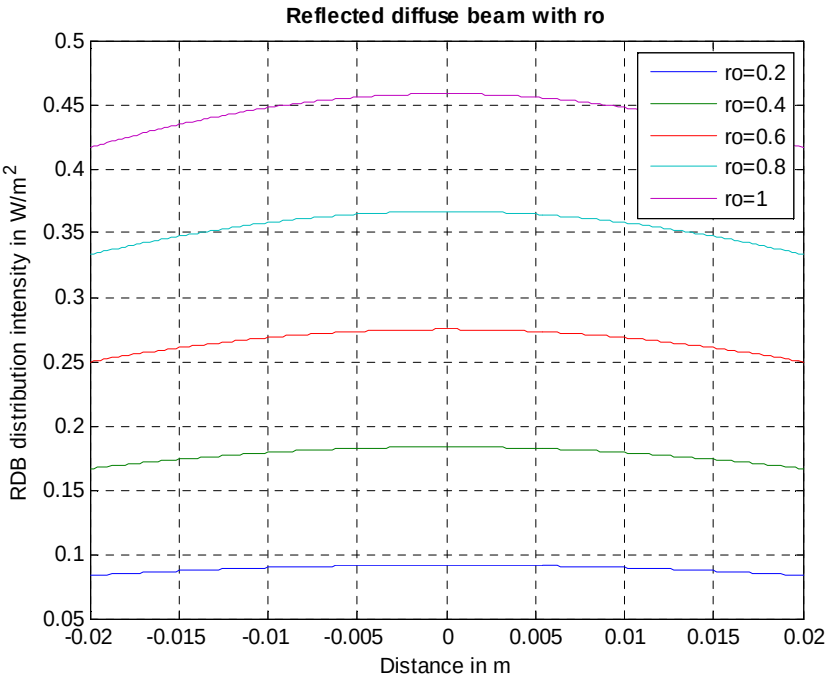

Fig.54. Reflected diffuse beam distribution and reflection coefficient

4.2.5. Intensity of Lambertian beam distribution

As in chapter 2 is already elaborated, intensity of Lambertian beam distribution stands as:

$$I(\phi) = \frac{m+1}{2\pi z^2} P cos^m(\phi) cos(\theta)$$

where *m* is the Lambertian order of radiation, ϕ is irradiance angle, θ is incident angle, and *z* is the transmission distance between source and receiver. For a given half power angle $\phi_{1/2}$, the Lambertian radiant order is:

$$m = -\frac{\ln(2)}{\ln(\cos\left(\phi_{\frac{1}{2}}\right))}$$

Considering the Lambertian beam as a part of diffuse beam, it is clear that the beam radius has a wide width. Suppose that the optical source has the Lambertian beam, in order to calculate the intensity of beam with its reflection. The intensity of Lambertian beam varies depending on the irradiance angle ϕ as an example fig.55 and fig.56 are shown. The intensity is in function of incident angle.

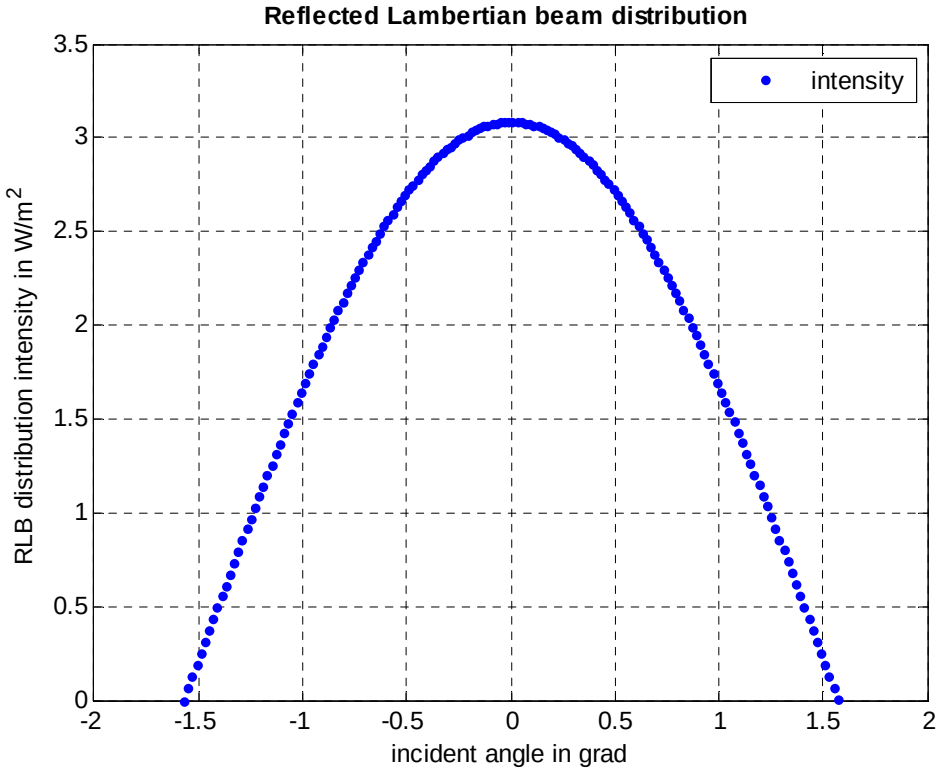

Fig.55. Reflected Lambertian beam distribution if $\phi=60^{o}$

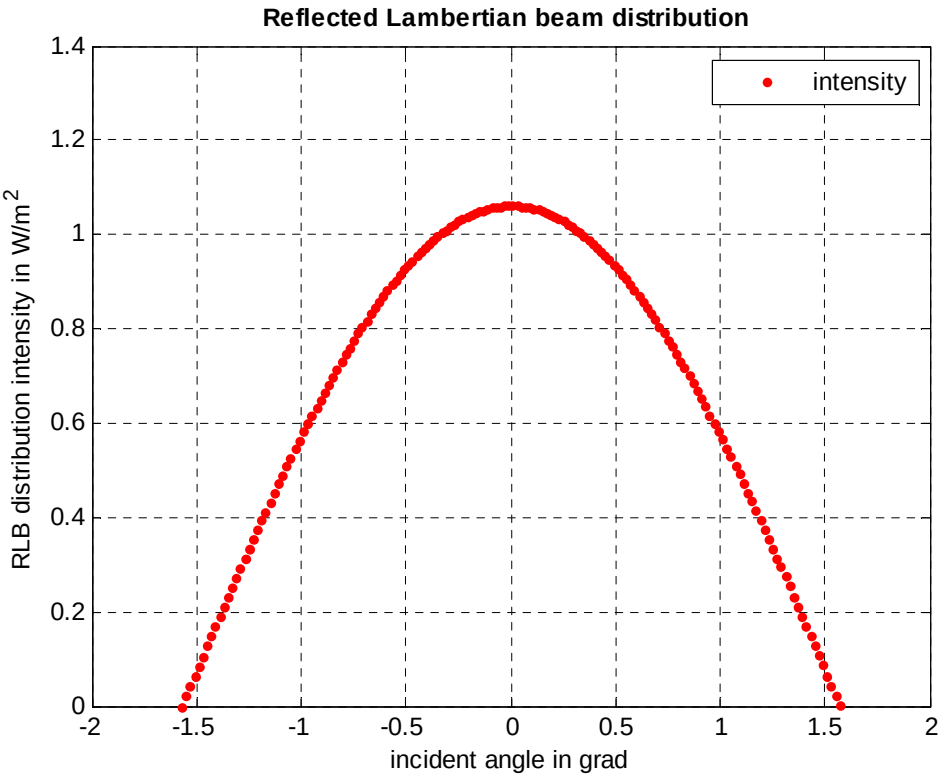

Fig.56. Reflected Lambertian beam distribution if $\phi=120$

5. Reflection-Analysis on Multiple Gaussian Beams

Until now the light beam (e.g. Gaussian and Lambertian beam) with single source has been demonstrated .But if the beam distribution has more than one optical source then light beam would be completely different. Again the equations of Gaussian distribution for each source are used. The beam intensity starts to increase using multiple sources. In other side the beam width radius becomes wider. Depending on number and positions of sources the beam takes a various form. In order to show the beam using four and eight optical sources, several examples are given in following sections.

5.1. Beam distribution and multiple sources in 3D

For this simulation task same parameters as before (in chapter 4) are used. In fig.57 an illustrated example of beam distribution with four sources as an array is given.

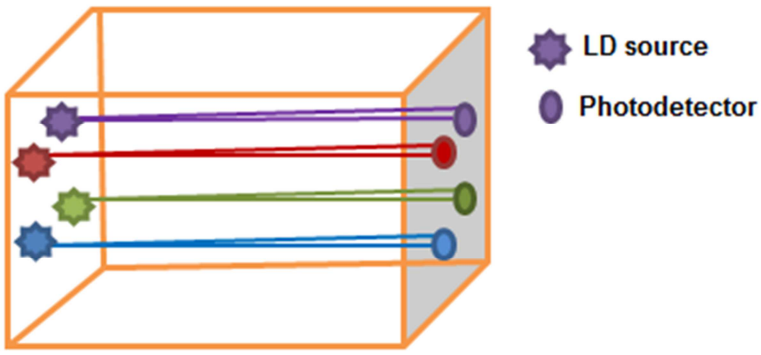

Fig.57. An illustration of beam distribution with multiple sources

Array of four transmitters (position coordinates in x-and y-direction (1,12), (12,1), (12,12), (1,1)) with a divergence angle 12.5^{o} are clearly shown in fig.58.

By changing divergence angle to 20^o a combination of four beams is given as shown in fig.59 (x- and y-coordinates (1,10), (10,1), (10,10), (1,1)). Variations of beams array and its reflection are demonstrated. Intensity of array varies with dependence of source coordination see fig.60 with x- and y-coordinates (6,12), (12,6), (3,6), (12,12).

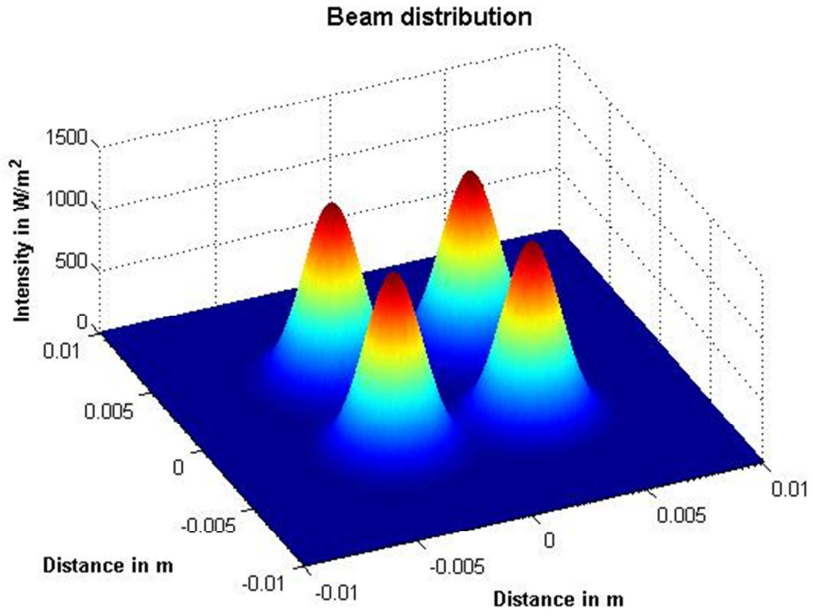

Fig.58. Beam distribution with 4 sources and divergence angle 12.5^o

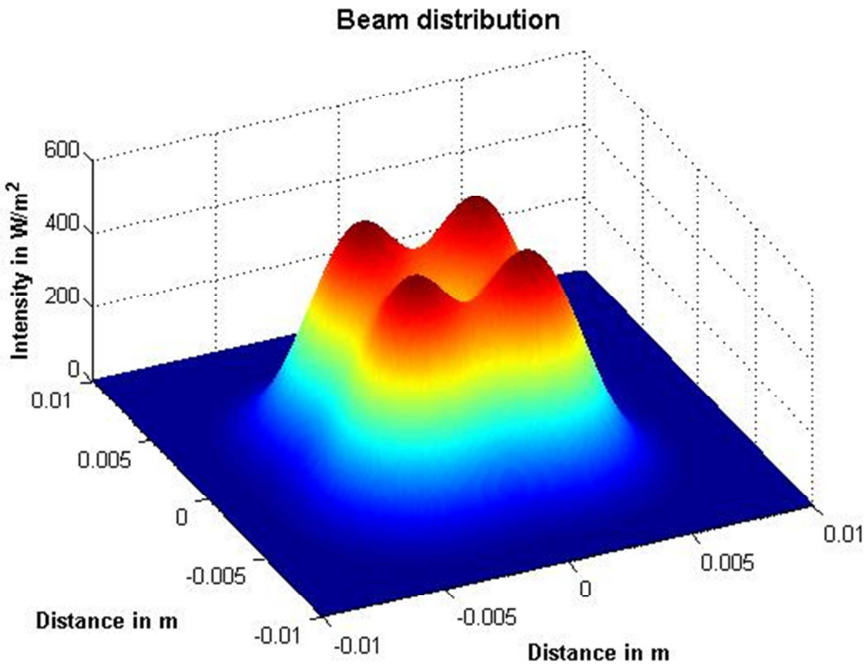

Fig.59. Beam distribution with 4 sources and divergence angle 20^o

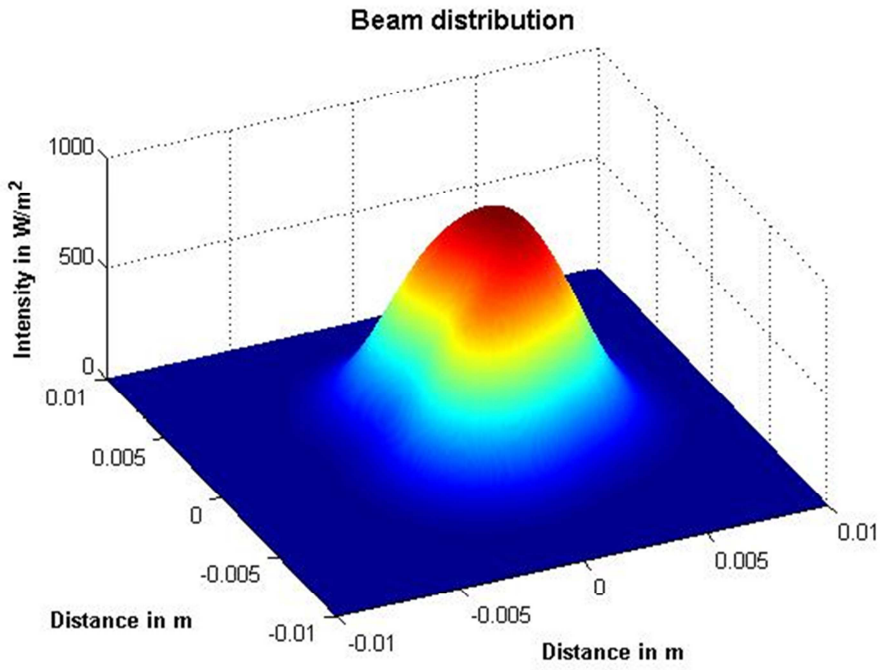

Fig.60. Beam distribution with 4 sources – case one

In the next two figures the reflected beam distributions are presented. Of course, the reflected beams indicate the lower value (fig.61 transmitters coordinates (1,10), (10,1), (10,10), (1,1) and fig.62 (6,12), (12,6), (3,6), (12,12)).

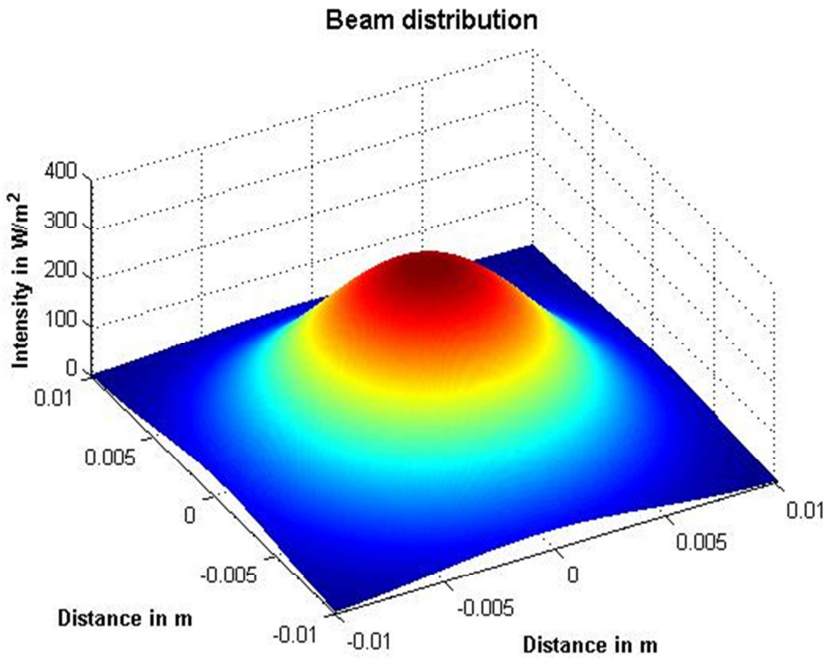

Fig.61. Reflected beam distribution with 4 sources – case one

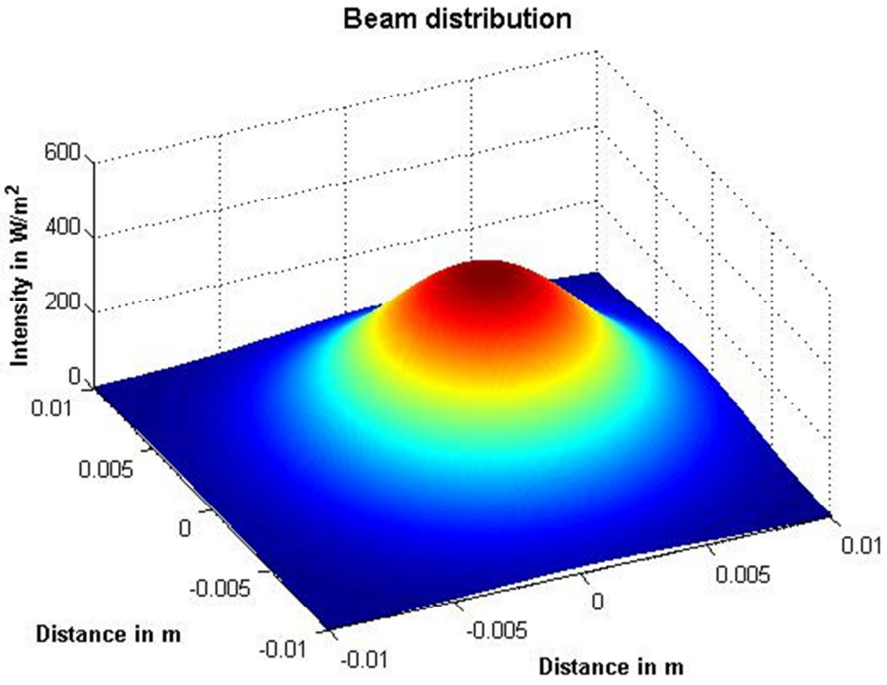

Fig.62. Reflected beam distribution with 4 sources – case two

5.2. Beam distribution with four transmitters

It is clear that changing of transmitters positions gives various intensity values. But, what if the LDs have a position in *x* or *y* line and each of them propagate light beams to the surface? Considering the positions of LDs, Gaussian beam takes various forms. It is also evident that when Gaussian beams multiple with each other than it is not Gaussian any more as shown in following.

5.2.1. Beam distribution with four transmitters in y-axis

Instead of one optical transmitter we use four transmitters. Positions of optical sources (LDs) are laying in y-axis see fig.63. There is a combination of four beam distributions or an array of beams.

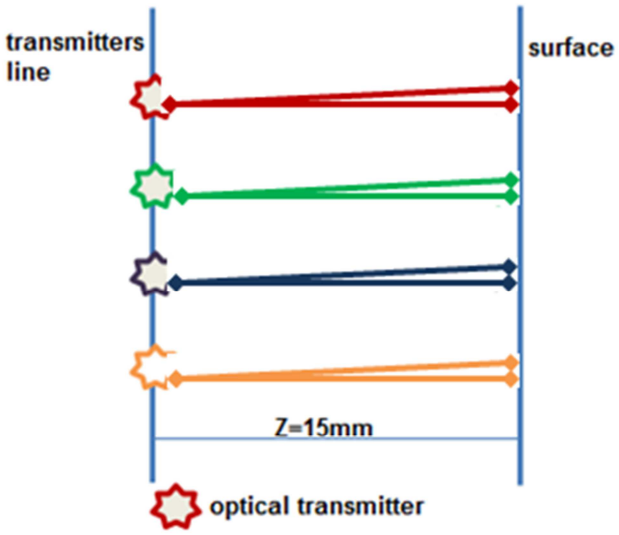

Fig.63. An illustration of beam distributions with 4 sources

In following figures examples we can see the difference between the beam distributions. For a single Gaussian beam the maximal intensity is 546 W/m^2, but the values of intensity increase using four optical beams. These values vary approximately from 600W/m^2 to 2200W/m^2. Fig.64 and Fig. 65 show beam distribution with position of sources in y direction (x- and y-coordinates (1,10), (1,8), (1,4), (1,2)) and (1,10), (1,8), (1,4), x(1,12)).

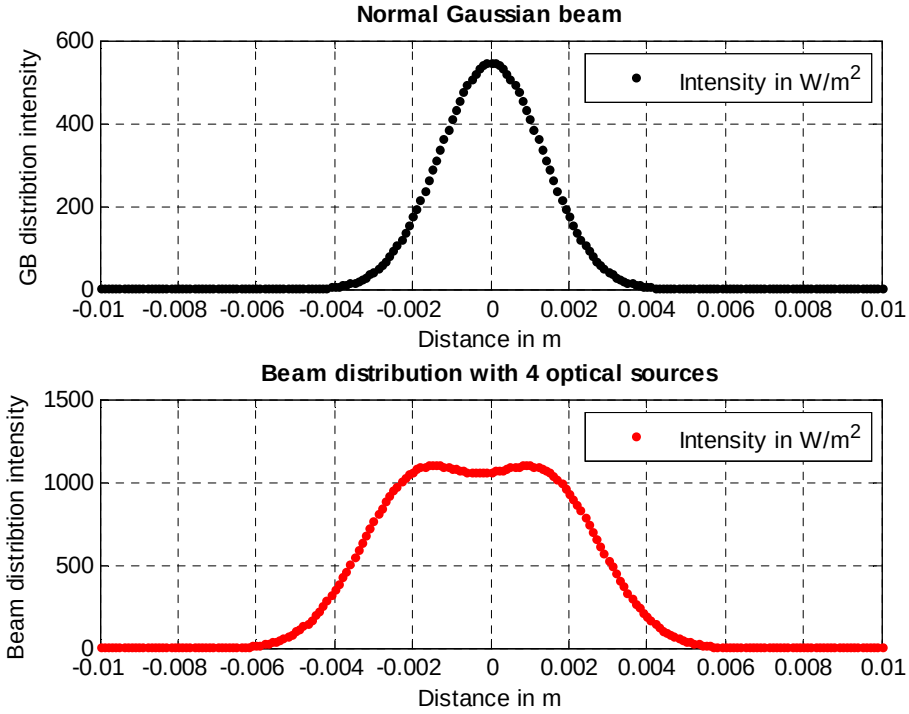

Fig.64. Beam distribution with 4 sources – first case

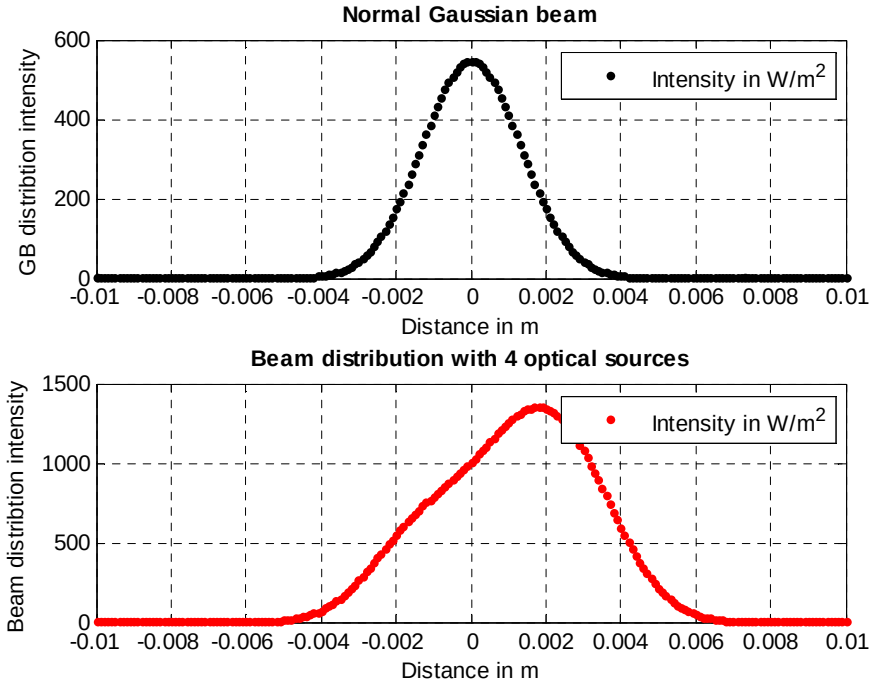

Fig.65. Beam distribution with 4 sources – second case

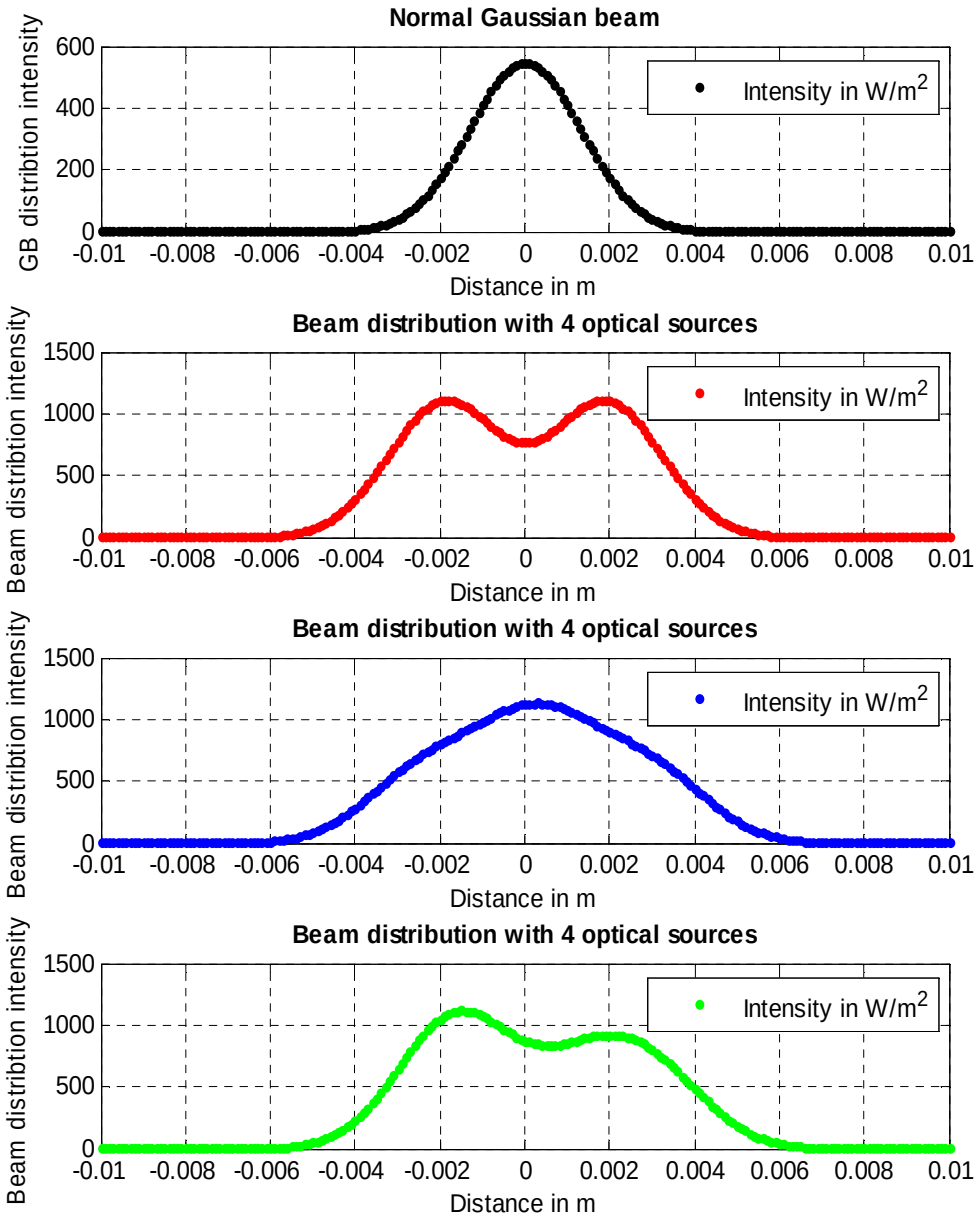

Fig.66. Other beam distributions with 4 sources laying in y-axis

5.2.2. Beam distribution with four transmitters and angle of incidence

Suppose that array of sources (in y-line) propagates the beam with an angle (e.g. 30 or 60 degree), the beam takes different forms considering the position of optical sources. The intensity decreases or increases in function of angle. Fig.67 shows array of beams shifted by an angle of 30 degree, where intensity reaches the value up to 800W/m^2 (x- and y-coordinates are (1,1), (1,2), (1,8), (1,12)). While for an angle of 60 degree, beam intensity reaches lower values (up to 300W/m^2) as shown in fig.68 (x- and y-coordinates are (1,1), (1,2), (1,8), (1,12)).

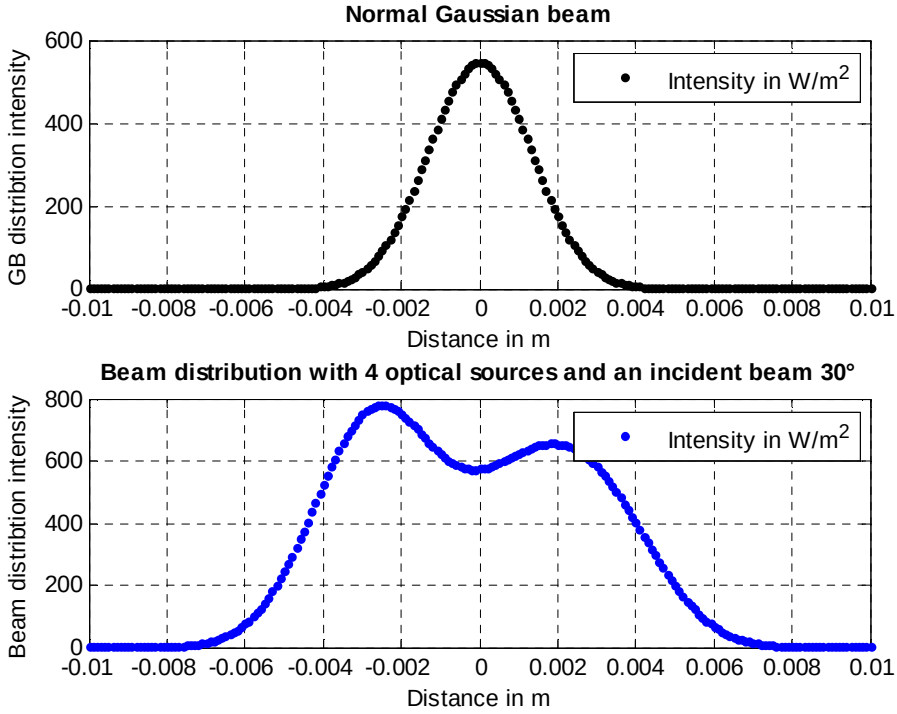

Fig.67. Beam distribution with 4 sources and incident angle 30^o

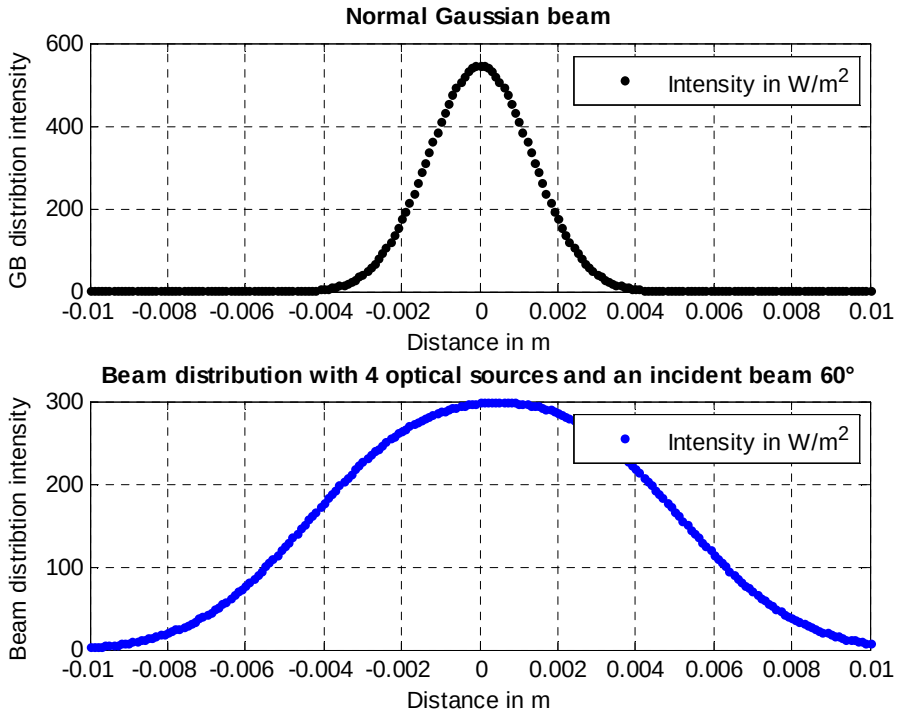

Fig.68. Beam distribution with 4 sources and incident angle 60^{o}

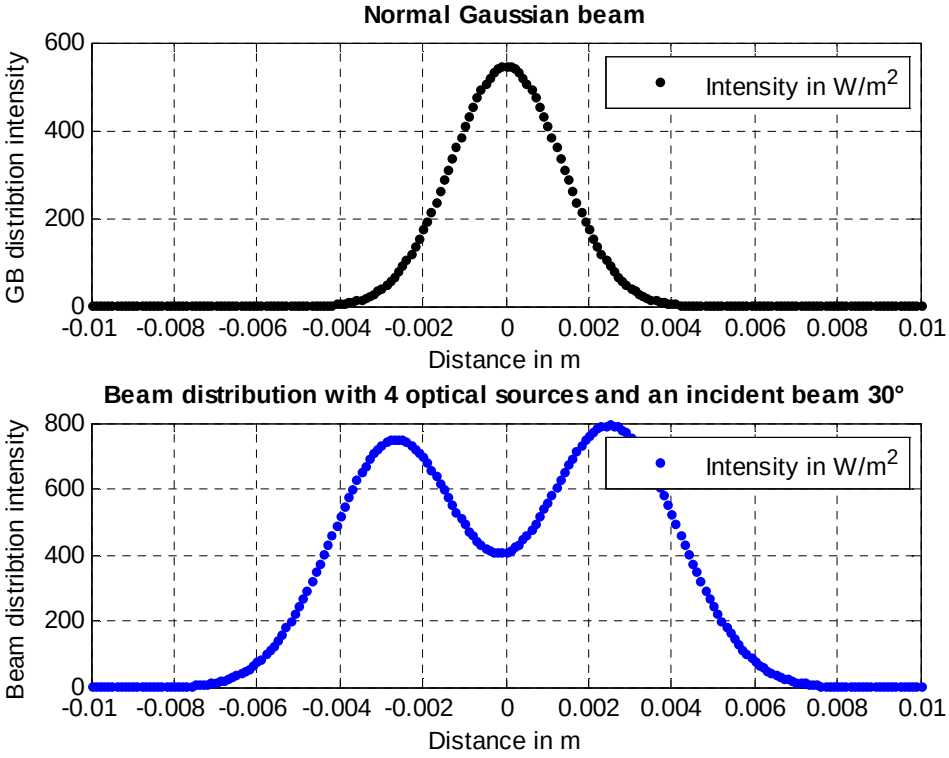

Fig.69. Beam distribution with 4 sources and incident angle 30^{o}

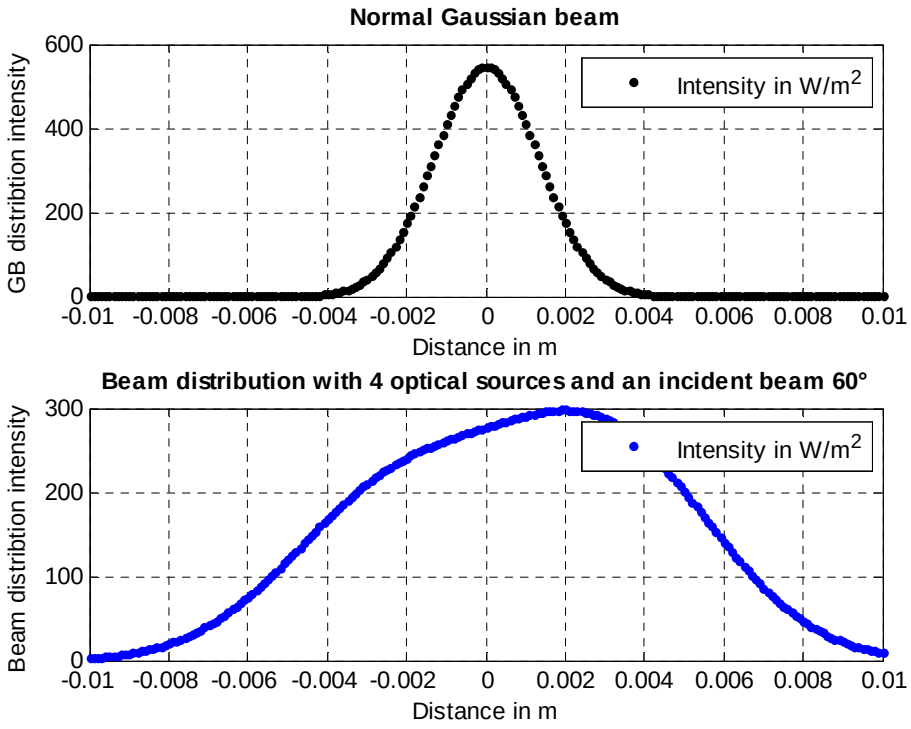

Fig.70. Beam distribution with 4 sources and incident angle 60^{o}

Fig.69 and fig.70 show array of beam distributions shifted by the angles 30 and 60 degree with positions of sources and x- and y-coordinates (1,10), (1,2), (1,12), (1,1).

5.3. Beam distribution with eight transmitters

In case of eight sources (y-line) the beam has also various distributions considering the positions of sources. The beam intensity shows higher values compare to the beam with four transmitters. The values of beam intensity vary depending on positions of transmitters. The examples of the beam distributions with eight optical sources are shown in following figures (see fig.71 positions coordinates (x- and y-coordinates are (1,1), (1,2), (1,4), (1,6), (1,8), (1,9), (1,10), (1,12), fig.72 other beam distribution and fig.73 beam distribution in 3D).

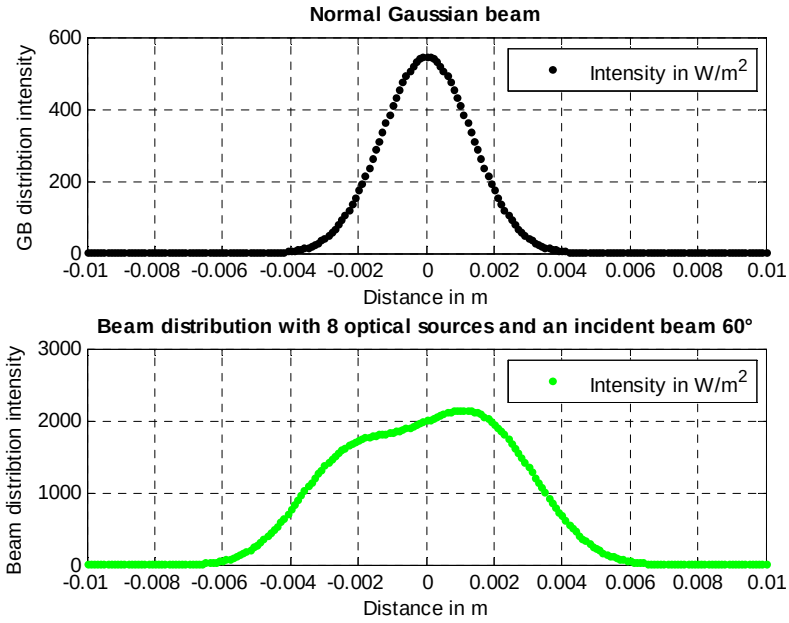

Fig.71. Beam distribution with 8 sources in y-axis

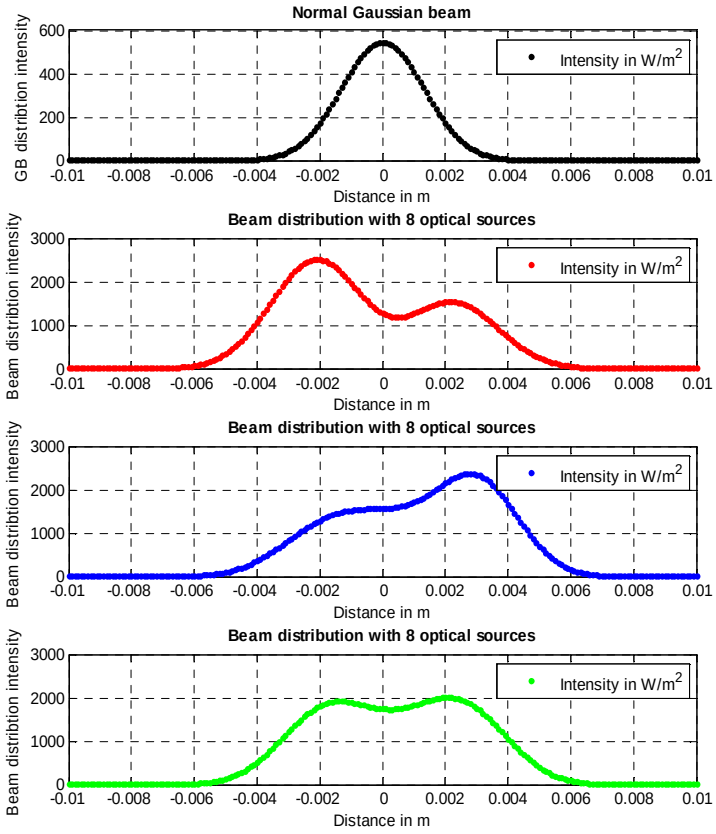

Fig.72. Other beams distributions with 8 sources in y-axis

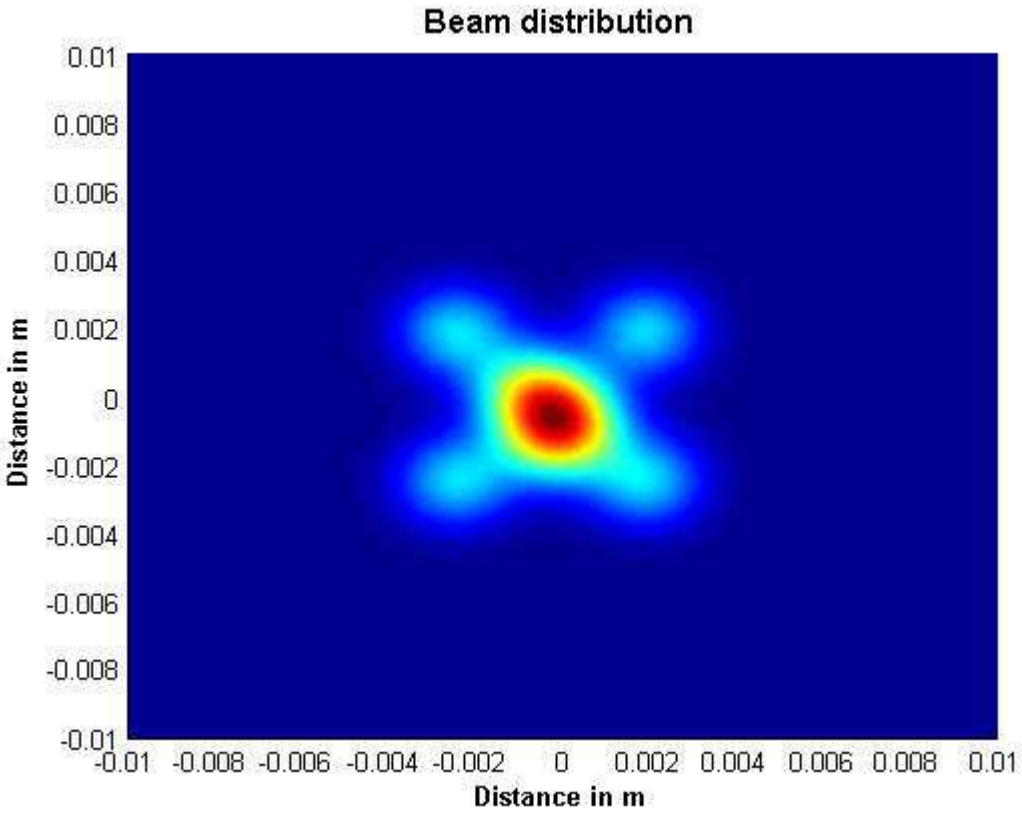

Fig.73. Beam distribution with 8 sources

6. Results

This chapter shows final simulation results considering the types of reflection's beam. The intensity of beam distribution using several methods and mathematical equations is calculated. Therefor the equations of Gaussian, diffuse and Lambertian beam distribution are expressed.

- First, the Gaussian beam distribution orthogonal to the mirror surface is simulated. It is clearly, a difference of the intensities and beam widths between incident beam and reflected beam. Second, different values of intensity are given, by varying the incident angle. Third, the influence of reflection coefficient is evident. Fourth, by varying the beam radius angle in *x* and *y* direction, elliptical Gaussian beam is formed.

- Reflected diffuse beam distribution is investigated. When the optical beam is perpendicular to the reflecting surface, the reflected diffuse beam is wider than in case of mirror surface. Assuming that scattering angle after reflection is higher than incident angle, the intensity would be lower.

- Beam distributions with multiple sources are analyzed. Each source is Gaussian distributed. The combination of more than one source gives various values of intensity. Examples of these beam distributions (2D and 3D) has been in chapter 5 presented.

In the table 8 the results of the reflected beam intensities (mirror I_{rg} and diffuse I_{rd}) using reflection coefficients ($\boldsymbol{r_o}$) are compared.

	r_o=0.2	r_o=0.4	r_o=0.6	r_o=0.8	r_o=1
I_{rdb} (W/m^2)	*0,0916789*	*0,183357*	*0,275036*	*0,3667156*	*0,4583946*
I_{rgb} (W/m^2)	*27,301173*	*54,60234*	*81,90352*	*109,20469*	*136,50586*

Table.9. Comparison of reflected intensities

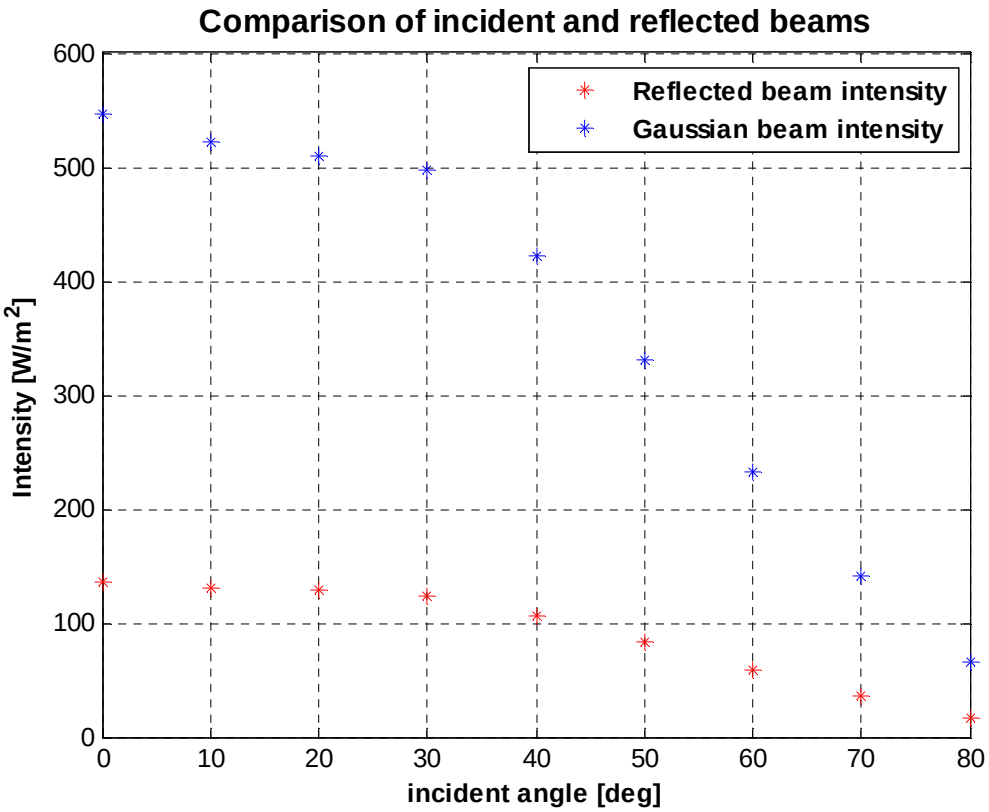

Fig.74. Intensities of incident and reflected beams

Fig.74 shows comparison between incident and reflected beams in function of an incident angle. It is seen that whenever the angle has great value, the beams intensities get lower values.

The situation of the beam distribution with multiple sources is different. Intensity of the beam distribution was higher compared to the one with single source. We saw in chapter 5 several variants of beam distributions. The values vary depending on number of sources, positions of sources and also in angle of incidence (as an array of sources).

7. Conclusion

In continuation with previous research papers on finding the methods and techniques to measure reflectivity in indoor environment, the focus of this work has addressed the attributes of the interaction between light and surface in short-range. Nowadays, there is a focus of researchers on connecting two devices through optical wireless link (high-speed data link). It is evident from simulation results, the importance of the optical beam reflections for application in optical link technology especially for High-Speed short distance optical wireless link.

In Chapter 4 the light beam (near IR) using mathematical and geometrical descriptions were demonstrated. The intensity of reflected beam varied depending on material surfaces and also on scattering angle. It is demonstrated that the presence of the various material surfaces (material with various refractive index) affects the light beam. The diversity of beams distributions plays a significant role for a direct and non-direct wireless link application. An example of this, Gaussian and diffuse beam distributions were presented. Chapter 5 indicated also a simulation method with multiple transmitters. The light beam using four and eight optical transmitters was demonstrated.

Infrared region is an attractive choice for many short-range applications (e.g. optical sensors for measurement, short-distance link applications etc.). One of the simulation's tasks that could challenge other simulation techniques is simulation of reflections with multiple sources. In this case, the simulation program would be able to calculate the irradiance distribution considering the position of transmitters and the reflecting points on the surface. The simulation programs or experimentally methods that would be also important for the short-range applications, is the simulation technique when the transmitter has different kinds of radiation beam.

Bibliography

Books:

[1] E.Leitgeb: *Optische Nachrichtentechnik*, Skriptum zur Vorlesung, TU Graz, 2009

[2] B. E. A. Saleh, Malvin Carl Teich, 1991: *Fundamentals of Photonics , John Wiley & Sons, Inc.* ISBNs: 0-471-83965-5 (Hardback); 0-471-2-1374-8 (Electronic)

[3] H.Haferkorn, *Optik* 3. Auflage 1994; Leipzig, Berlin, Heidelberg, Barth, ISBN 3-335-00363-2

[4] F.Pedrotti, L.Pedrotti, W.Bausch, H.Schmidt, *Optik für Ingenieure Grundlagen 2.Auflage:* 2002, ISBN 3-540-67379-2

[5] T.-Chung P., T.Kim, *Engineering Optics with Matlab*, 2006 by World Scientific Publishing Co. Pte. Ltd, ISBN 981-256-872-7

[6] Z. Ghassemlooy, W. Popoola, S. Rajbhandari: *Optical Wireless Communications System and Channel Modelling with MATLAB,* 2013 by Taylor & Francis Group, LLC, International Standard Book Number-13: 978-1-4398-5235-4

[7] M. J. Weber, Ph.D., Berkeley, California: *Handbook of optical materials* 2003 by CRC Press LLC

[8] E.Hecht *Optics 1997*

[9] R.D. Guenther, *Modern Optics John Wiley & Sons 1990* ISBN: 0471605387

[10] M. Bass, E. W. Van Stryland, D.R . Williams, W. L . Wolfe: *HANDBOOK OF OPTICS* 1995, Sponsored by the OPTICAL SOCIETY OF AMERICA, ISBN 0-07-047974-7

[11] R.S. Quimbly Photonics and Lasers: An Introduction John & Wiley, Inc. 2006

Journal papers:

[12] J. Vitásek, P. Koudelka, Ing. J.Látal, F. Dostál, K. Sokanský: *Indoor optical free space network - reflectivity of light on building materials*. -TU Ostrava, Faculty of Electrical Engineering and Computer Science, ISSN 0033-2097, R. 87 NR 4/2011

[13] P.Hrbackova, O.Wilfert: *Model for indoor wirless optical link,* Doctoral degree Program (1) FEEC BUT . No. FEKT_S_10_9. 2011.

[14] O.Wilfert, A.Prokes, J.Diblik, P. Herbackova: Power budget model for indoor wireless optical link. Insittute of radion Electronics, Brno University of Technology, Purkynova 118, 612 00 Brno (Czech Republic). Proc. of SPIE Vol. 8162 81620W-3 , 2011.

[15] Z.Ghassemlooy, Senior Member, IEEE, S. Rajbhandari, Member, IEEE, Hoa Le Minh, Member, IEEE and A. C. Boucouvalas, *Improvement of Transmission Bandwidth for Indoor Optical Wireless Communication Systems Using a Diffuse Gaussian Beam*, Dehao Wu, Student Member, Fellow, VOL. 16, NO. 8, AUGUST 2012

[16] Z. Ghassemlooy, Senior Member, IEEE, S. Rajbhandari, Member, IEEE, Hoa Le Minh, Member, IEEE and A. C. Boucouvalas, *Improvement of Transmission Bandwidth for Indoor Optical Wireless Communication Systems Using an Elliptical Lambertian Beam* Digital Object Identifier : 10.1109/LPT.2012.2227304, 15 November 2012.

[17] F..A. Al-Bassam: *The near infrared reflective materials surfaces : dimensions and angles*. J. of university of anbar for pure science : Vol.3: No.2 : 2009

[18] J. M. KAHN, JOHN R. BARRY: *Wireless Infrared Communications.* PROCEEDINGS OF THE IEEE, VOL. 85, NO. 2, FEBRUARY 1997

[19] K. Lee, H. Park, and J. R. Barry, "Indoor Channel Characteristics for Visible Light Communications," Communications Letters, IEEE, vol. 15, pp. 217-219, 2011.

[20] J. Poliak, P. Pezzei, E. Leitgeb and O.Wilfert, *Analytical Expression of FSO Link Misalignments Considering Gaussian Beam* Institute of Radio Electronics, Brno University of Technology, Purkyova 118, 612 00 Brno, Czech Republic Institute of Microwave and Photonic Engineering, Graz University of Technology, Inffeldgasse 12, Graz, Austria NOC/OC&I 2013, ISBN: 978-1-4673-5822-4

[21] J.Poliak, P. Pezzei, E. Leitgeb and O. Wilfert, *Link budget for high-speed short-distance wireless optical link* Institute of Radio Electronics, Brno University of Technology, Purkyova 118, 612 00 Brno, Czech Republic Institute of Microwave and Photonic Engineering, Graz University of Technology, Inffeldgasse 12, Graz, Austria, 978-1-4577-1473-3/12/$26.00 ©2012 IEEE

[22] Petrov, V. A., REFLECTION COEFFICIENT (REFLECTANCE) 7 February 2011, 10.1615/AtoZ.r.reflection_coefficient_reflectance, viewed 11.06.2014 16:30.

[23] A. Vijay, Member, IEEE Roger.J.Green, Senior Member, IEEE : *Channel Models for Radio on Visible (RoVL) Communication System.* School of Engineering, University of Warwick, Coventry, CV4 7AL, England. ICTON 2014.

[24] T. DAVID, J. LATAL, F. HANACEK, P. KOUDELKA, J. VITASEK, P. SISKA, J. SKAPA, V. VASINEK: *CROSS-SECTIONAL MEASURING OF OPTICAL BEAM* Department of Telecommunications, Faculty of Electrical Engineering and Computer Science, VSB – Technical, 2011 ADVANCES IN ELECTRICAL AND ELECTRONIC ENGINEERING University of Ostrava, 17. listopadu 15, 708 33 Ostrava, Czech Republic

[25] H.Q. Nguyen, J.-H. Choi, M. Kang, Z. Ghassemlooy, D. H. Kim, S.-K. Lim, T.-G. Kang, and C. G. Lee, *A MATLAB-based simulation program for in-*

door visible light communication system . Northumbria University, United Kingdom LED Communication Research Team, ETRI, South Korea, Communication Systems Networks and Digital Signal Processing (CSNDSP), 2010 7th International Symposium 21-23 July 2010, Print ISBN:978-1-4244-8858-2

[26] P.Konieczny, A.Woiska, J. Swiderski, A.Zajac: *Simulation of reflected and scattered laser radiation for designing laser shields* (JOSE) 2008 Vol.14,No.2. 133-147 Warszawn, Poland E. Sarbazi,

[27] M. Uysal, M. Abdallah and K. Qaraqe *Indoor Channel Modeling and Characterization for Visible Light Communications* Department of Electrical and Electronics Engineering, Ozyegin University, Istanbul, Turkey Electrical and Computer Engineering, Texas A&M University, Doha, Qatar ICTON 2014

[28] T. ŞEN - REFLECTION PROPERTIES OF A GAUSSIAN LASER BEAM FROM MULTILAYER DIELECTRIC FILMS, *İzmir Institute of Technology December, 2009 Thesis*

Website sources:

[29] http://www.colorado.edu/physics/phys4510/phys4510_fa05/Chapter5.pdf (viewed 11.05.2014)

[30] http://www.pololu.com/product/2458 : *QTR-1A Reflectance Sensor* Robotics and electronics Pololu 17.06.2014 (15:22)

[31] http://mathworld.wolfram.com/RightTriangle.html (viewed 18.06.2014)

[32] www.shoelacescience.com , LossMeter Application Note

[33] http://www.4physics.com/tn3/lambertian.htm (viewed 22.06.2014)

[34] http://www.mathworks.com, MATLAB description (viewed 25.06.2014)

[35] P. Pezzei, E.Leitgeb: *Power distribution of short free space optical propagation* TUGraz, ICTON 2014

List of Figures

Figure 1: QTR-1A Reflectance Sensor..... 3

Figure 2: Loss Meter metrology instrument..... 4

Figure 3: Decay curve of a linear cavity from a CW-laser (1315 nm)..... 5

Figure 4: Block diagram of measuring system of directional characteristics. 6

Figure 5: The samples of coatings. 6

Figure 6: The samples of building and tiling materials. 7

Figure 7: Directional characteristic of a) sample no.6 and b) no.13 (650 nm).... 8

Figure 8: Directional characteristic of sample no.6, wavelength 850 nm..... 8

Figure 9: Directed line-of-sight (LOS) ray geometry for mobile telephony..... 9

Figure 10: Diffuse ray geometry for mobile telephony through visible light. 9

Figure 11: Received optical power for 3 bounces - Infrared case. 10

Figure 12: Received optical power for 3 bounces - visible light case. 11

Figure 13: The basic principle of the RDR measurement..... 14

Figure 14: Optical wireless LANs: a) diffuse link and b) line of sight.. 14

Figure 15: Types of reflection..... 15

Figure 16: Geometry of the propagation vectors..... 16

Figure 17: Reflection factor with TE polarization..... 17

Figure 18: Electrical reflection factor with TE-polarization and incident angle . 20

Figure 19: Reflection factor with TM polarization. 20

Figure 20: Interpretation of the Brewster effect. 23

Figure 21: Electrical reflection factor with TM-polarization and incident angle. 24

Figure 22: Reflection and transmission coefficients (real part)..... 25

Figure 23: Magnitude of coefficients vs. incident angle..... 25

Figure 24: Phase angle of coefficients vs. incident angle..... 26

Figure 25: Beam waist radius and radius of curvature 28

Figure 26: Beam spreading angle. 29

Figure 27: Gaussian beam profile. 30

Figure 28: Intensity of Gaussian beam distribution. 31

Figure 29: Gaussian beam distribution through a diffuser. 33

Figure 30: Gaussian beam distribution through a diffuser in a room. 34

Figure 31: Distribution of illuminance in case of one transmitter 35

Figure 32: Illuminance distribution with 4 transmitters and semi angle of 30^o. . 36

Figure 33: Illuminance distribution with 4 transmitters and semi angle of 70^o. . 36

Figure 34: Gaussian beam distribution and reflection from mirror surface. 39

Figure 35: Gaussian beam distribution..... 40

Figure 36: Reflected Gaussian beam distribution..... 40

Figure 37: An illustration of multiple reflections 41

Figure 38: Intensity distribution after second reflection (green) 42

Figure 39: Intensity distribution after third reflection (orange) 42

Figure 40: An illustration of light beam with an incident angle φ. 43

Figure 41: Illustration of reflection with an incident angle φ..... 45

Figure 42: Gaussian beam distribution with an incident angle 30^o 46

Figure 43: Gaussian beam distribution with an incident angle 60^o 46

Figure 44: Gaussian beam distribution with an incident angle 70^o 47

Figure 45: RGB distribution with an incident angle 30 and multiple reflections. 47

Figure 46: Gaussian beam with reflectivity (*ro*=0.2, 0.4, 0.6, 0.8, 1) 48

Figure 47: Circular form of reflected Gaussian beam distribution ($\theta_x = \theta_y$)..... 49

Figure 48: Elliptical reflected beam a) $\theta_x = 15°, \theta_y = 5°$ and b) $\theta_x = 5°, \theta_y = 15°$. 50

Figure 49: An illustration of diffuse beam distribution. 51

Figure 50: Comparison of the beam waist radii. 52

Figure 51: RDR in function of scattering angle. 53
Figure 52: Reflected diffuse beam distribution if ϕ=60˚ 54
Figure 53: Reflected diffuse beam distribution if ϕ=120˚ 55
Figure 54: Reflected diffuse beam distribution and reflection coefficient 56
Figure 55: Reflected Lambertian beam distribution if ϕ=60˚ 57
Figure 56: Reflected Lambertian beam distribution if ϕ=120˚ 58
Figure 57: An illustration of beam distribution with multiple sources 59
Figure 58: Beam distribution with 4 sources and divergence angle 12.5^{o} 60
Figure 59: Beam distribution with 4 sources and divergence angle 20^{o} 60
Figure 60: Beam distribution with 4 sources - case one 61
Figure 61: Reflected beam distribution with 4 sources - case one 61
Figure 62: Reflected beam distribution with 4 sources - case two 62
Figure 63: An illustration of beam distributions with 4 sources 63
Figure 64: Beam distribution with 4 sources first case 64
Figure 65: Beam distribution with 4 sources second case 64
Figure 66: Other beam distributions with 4 sources laying in y direction 65
Figure 67: Beam distribution with 4 sources and incident angle 30^{o} 66
Figure 68: Beam distribution with 4 sources and incident angle 60^{o} 67
Figure 69: Beam distribution with 4 sources and incident angle 30^{o} 67
Figure 70: Beam distribution with 4 sources and incident angle 60^{o} 68
Figure 71: Beam distribution with 8 sources in y-direction 69
Figure 72: Other beams distributions with 8 sources in y-direction 69
Figure 73: Beam distribution with 8 sources 70
Figure 74: Intensities of incident and reflected beams 72

List of Tables

Table 1: The description of samples of coatings **[12]** 7

Table 2: The samples of building and tiling materials **[12]** 7

Table 3: Designation of radiation **[1]** 13

Table 4: Reflectance of the mirror metals **[3]** 37

Table 5: Specifications for simulation of the optical beam 39

Table 6: Specifications for simulation of the optical beam adding reflectivity .. 48

Table 7: Beam radii in function of distances (in mm) 52

Table 8: Specifications for reflected diffuse beam distribution 54

Table 9: Comparison of reflected intensities 71

List of Abbreviations

IWOL – indoor wireless optical link

FSO – free space optic

RDR – relative directional reflectivity

TE – electrically transverse

TM – magnetically transverse

GB – Gaussian beam

RGB – reflected Gaussian beam

DB – diffuse beam

RDB – reflected diffuse beam

LB – Lambertian beam

RLB – reflected Lambertian beam

LED – light-emitting diode

CW – continuous wave

RoVL – radio on visible light communication

LOS – line of sight

NLOS – non-line of sight

IR - Infrared

LSD – light shaping diffuser

LD – laser diode

FWHM – full width at half maximum

Appendix A: Gaussian beam with reflections

```
%% Gaussian beam distribution
%
%
% Date: 2013/12/17
% Author: Krenar Rexhepi
% Research Group: Master's thesis
% Institute: Institute for microwaves and photonics
% University: Graz university of technology
%
%% -------------------- BEGIN CODE --------------------
clear all
close all
clc

%% Specifications and constants
Theta = 20;                 % Full divergence angle in grad
lambda = 850e-9;            % Wavelength in m
z = 15*10^-3;               % Distance in m
P_t = 0.006;                % Total power in Watt of a light source
%% General calculations


alpha = Theta * pi / (180 *2);          % Half divergence angle in
rad
betta = (90-Theta/2)*pi/(180);          % Angle calculated from sum
of 90° and alpha (Theta/2)
                                        % Calculate angle from re-
flection's law
gamma = (180*pi/(180)-2*betta);         % Full reflected divergence
angle in radius


%% 1) Linear beam radius
w_z = z * tan(alpha);                   % Constant beam radius in m




%% 2) Total intensity of gaussian distribution in W/m^2

[X, Y] = meshgrid(-0.01:.0001:0.01, -0.01:.0001:0.01)

I_0 = 2*P_t/(pi*(w_z)^2);                                       % Maxi-
mal intensity of gaussian in distribution in W/m^2
I_gauss = I_0*exp((-X.^2-Y.^2)/(w_z^2));                        % Total
intensity of gaussian distribution in W/m^2
```

```
%% 3) Reflected beam radius

z1 = z+15*10^-3;

w_zr = z1*tan(alpha);                                          % Re-
flected beam width radius in m


%% 4) Total Intensity of reflected gaussian distribution in W/m^2

[X, Y] = meshgrid(-0.01:.0001:0.01, -0.01:.0001:0.01)

I_0r = 2*P_t/(pi*(w_zr)^2);                                     % Maxi-
mal intensity of reflected gaussian distribution in W/m^2
I_ref = I_0r*exp((-X.^2-Y.^2)/(w_zr^2));                        % Total
intensity of reflected gaussian distribution in W/m^2




%% Graph
figure
surf(X,Y,I_ref);
view (-25,50)
shading interp;
title('Reflected Gaussian beam','Fontsize', 12,'FontWeight','bold');
xlabel('Distance in m','FontWeight','bold');
ylabel('Distance in m','FontWeight','bold');
zlabel('Reflected Gaussian distribtion intensi-
ty','FontWeight','bold');
figure
surf ( X,Y,I_gauss);
shading interp;
view (-25,50)
title('Gaussian beam','Fontsize', 12,'FontWeight','bold');
xlabel('Distance in m','FontWeight','bold');
ylabel('Distance in m','FontWeight','bold');
zlabel('Gaussian distribution intensity','FontWeight','bold');
```

```
%% Gaussian beam propagation and reflection
%
%
% Date: 2013/05/17
%
% Author: Krenar Rexhepi
% Research Group: Master's thesis
% Institute: Institute for microwaves and photonics
% University: Graz University of Technology
%
%% -------------------- BEGIN CODE --------------------
clear all
close all
clc

%% Specifications and constants
```

```
Theta = 20;                 % Full divergence angle in grad
lambda = 850e-9;            % Wavelength in m
z = 15*10^-3;               % Distance in m
P_t = 0.006;                % Total power in Watt of a light source

%% General calculations


alpha = Theta * pi / (180 *2);           % Half divergence angle in
rad

phi = -60*pi / (180);                     % Rotated angle in rad

ymin = z*tan(phi-alpha);
ym=z*tan(phi);
ymax=z*tan(phi+alpha);

a1 = sqrt(z^2+ymin^2);
a2 = sqrt(z^2+ymax^2);


z1 = z/cos(phi);
z2_min = a1*cos(alpha);
z2_max = a2*cos(alpha);


z2 = linspace(z2_min,z2_max,201);

%% 1) Linear beam radius
w_z = z * tan(alpha);                      % Constant beam radius in m
w_z0 = z1*tan(alpha);                      % new beam width radius of
spreading beam in m
w_z1 = 2*z1*tan(alpha);                    % new beam width radius of
reflected beam in m
w_z2 = z2.*tan(alpha);                     % vector of beam width ra-
dius of spreading beam
w_z3 = 2*z2.*tan(alpha);                   % vector of beam width ra-
dius of reflected beam


%% 2) Total intesity of gaussian distribution in W/m^2

P_t = 0.006*ones(size(z2));
% Total power in Watt of a light source



r = linspace(-0.01,0.01,201);



I_0 = 2*P_t./(pi*(w_z2).^2);
% Maximal intesity of Phase-shifted Gaussian distribution in W/m^2
I_gauss = I_0.*exp((-2*(r.^2)/(w_z0^2)));
% Total intesity of Phase-shifted Gaussian distribution in W/m^2
```

```
I_00 = 2*P_t./(pi*(w_z3).^2);
% Maximal intesity of Phase-shifted Reflected Gaussian beam distribu-
tion in W/m^2
I_gauss1 = I_00.*exp((-2*(r.^2)/(w_z1^2)));
% Total intesity of  Phase-shifted Reflected Gaussian beam in W/m^2


%% Graph

figure
subplot(2,1,1)
plot(r,I_gauss,'k.','MarkerSize',10);
title('Gaussian beam with angle 60°','FontWeight','bold');
xlabel('Distance in m');
ylabel('GB distribtion intensity');
legend ('Intensity in W/m^2');
grid on
subplot(2,1,2)
plot(r,I_gauss1,'k.','MarkerSize',10,'Color','blue');
title('Reflected Gaussian beam with angle 60°','FontWeight','bold');
xlabel('Distance in m');
ylabel('RGB distribtion intensity');
legend ('Intensity in W/m^2');
grid on
```

```
%% Reflected Gaussian beam propagation with reflection coefficients
%
%
% Date: 2013/05/17
%
%
% Author: Krenar Rexhepi
% Research Group: Master's thesis
% Institute: Institute for microwaves and photonics
% University: Graz university of technology
%
%% -------------------- BEGIN CODE --------------------
clear all
close all
clc

%% Specifications and constants
Theta = 20;                 % Full divergence angle in grad
lambda = 850e-9;            % Wavelength in m
z = 15*10^-3;               % Distance in m
P_t = 0.006;                % Total power of optical source
ro = [0.2 0.4 0.6 0.8 1];   % Reflectivity
%% General calculations


alpha = Theta * pi / (180 *2);          % Half divergence angle in
rad

gama = 60*pi/180;
```

```
%% 1) Reflected beam radius

w_z = z * tan(alpha);                       % Reflected beam radius in m



%% 2) Total intesity of gaussian distribution in W/m^2

r = (-0.01:0.0001:0.01);

N = length(r);
M = length(ro)




for i = 1 : N;
    for j = 1 : M;
        I_0 = 2*P_t*ro(j)/(pi*(w_z)^2);                          % max-
imal Intensity I_0 in W/m^2
        I(i,j) = I_0*exp(-2* ( (r(i)^2 /w_z^)2 ));               % In-
tensity of Gaussian distribution in W/m^2
    end
end

%% Graph
figure
plot(r,I);
title('Reflected Gaussian beam with angle 60° and different
ro','FontWeight','bold');
xlabel('Distance in m');
ylabel('RGB distribution intensity');
legend ('ro=0.2', 'ro=0.4','ro=0.6','ro=0.8','ro=1');
grid on
```

Appendix B: Diffuse beam distribution

```
%% Diffuse beam distribution
%
% Date: 2014/05/17
% Author: Krenar Rexhepi
% Research: Master's thesis
% Based on jurnal paper: Improvement of Transmission bandwidth for
IOWC systems using diffused Gaussian beam
% Institute: Institute for microwaves and photonics
% University: Graz university of technology
%% -------------------- BEGIN CODE --------------------
clear all
close all
clc

%% Specifications and constants
Theta = 20;                 % Full divergence angle in grad
lambda = 850e-9;            % Wavelength in m
z = 15*10^-3;               % Distance in m
Phi = 120;                  % Reflected diffuse angle
P_tx = 0.006;
%% General calculations
alpha = Theta * pi / (180 *2);         % Half divergence angle in rad

beta = Phi * pi / (180 *2);            % Half reflected diffuse angle
in rad

%% 1) beam radius
w_z = z*tan(alpha);                       % Constant beam radius in m

w_z1 = 2*sqrt(2/log(2))*z*tan(beta);      % Diffused beam radius in m
(from Digital Object Identifier: 10.1109/LCOMM.2012.060812.120803
equation (6))

%% 2) intensity of gaussian beam distribution in W/m^2
[X,Y]=meshgrid(-0.01:0.0001:0.01,-0.01:0.0001:0.01);


I_0 = 2 * P_tx / (pi * w_z^2);
I_gb=I_0*exp(-2*(X.^2+Y.^2)/(w_z^2))

%% 3) intensity of diffused beam distribution in W/m^2

[X,Y]=meshgrid(-0.01:0.0001:0.01,-0.01:0.0001:0.01);


I_01 = 2 * P_tx / (pi * w_z1^2);
I_db = I_01*exp(-2*(X.^2+Y.^2)/(w_z1^2))

%% graph
```

```
figure
surf(X,Y,I_gb);
title('Gaussian beam','FontWeight','bold');
xlabel('Distance in m');
ylabel('Distance in m');
zlabel('Intensity in W/m^2');
shading interp;
view(-30,46)
colorbar;
figure
surf(X,Y,I_db);
title('Reflected Diffuse beam','FontWeight','bold');
xlabel('Distance in m');
ylabel('Distance in m');
zlabel('Intensity in W/m^2');
shading interp;
view(-30,46)
colorbar
```

Appendix C: Lambertian beam distribution

```
%% Lambertian beam
%
%
% Date: 2014/05/17
% Author: Krenar Rexhepi
% Research Group: Master's thesis
% Institute: Institute for microwaves and photonics
% University: Graz university of technology
%
%% -------------------- BEGIN CODE --------------------
clear all
close all
clc

%% Specifications and constants
lambda = 850e-9;            % Wavelength in m
z = 15*10^-3;               % Distance in m
P_t = 0.006;                % Total power of optical source
ro = [0.2 0.4 0.6 0.8 1];   % Reflectivity
Phi = 120;                   % Full width divergence angle of a Lam-
bertian optical source in grad
%% General calculations


beta = Phi * pi / (180 *2);            % Half divergence angle in rad

a = -log(2)*ones(size(beta));

m=a./log(cos(beta));                   % Lambertian order of emission

gama = 90*pi/180;

%% 1) Reflected-Diffused beam radius

w_z1 = 2*z*tan(beta);                  % Reflected Lambertian beam
waist radius (from Digital Object Identifier: 10.1109/LPT.2012.2227304
equation (4))


%% 2)  Intensity of reflected Lambertian beam distribution in W/m^2

[r] = (-gama:0.02:gama)

I_0 = P_t*((m+1)/(2*pi*(2*z)^2))*cos(beta)^m;            % Maximum in-
tensity of Lambertian beam distribution
I = I_0*cos(r);                                          % Intensity
of Lambertian beam distribution in W/m^2(from Digital Object Identifi-
er: 10.1109/LPT.2012.2227304 equation (1))
```

```
%% Graph

figure

plot(r,I,'k.','MarkerSize',10,'Color','blue');
title('Reflected Lambertian beam distribution ','FontWeight','bold');
xlabel('incident angle in grad');
ylabel('RLB distribution intensity in W/m^2');
legend ('intensity');
grid on
```

Appendix D: Beam distribution with multiple sources

```
%% Beam distribution with multiple sources
%
%
% Date: 2014/09/17
% Version: 1.0
%
% Author: Krenar Rexhepi
% Research Group: Master's thesis
% Institute: Institute for microwaves and photonics
% University: Graz university of technology
%
%% -------------------- BEGIN CODE --------------------
clear all
close all
clc

%% Specifications and constants
Theta = 20;                 % Full divergence angle in grad
lambda = 850e-9;            % Wavelength in m
z = 15*10^-3;               % Distance in m
P_tx = 0.006;

%% General calculations


alpha = Theta * pi / (180 *2);           % Half divergence angle in
rad

phi = -0*pi / (180);                    % LEDSource-incident angle in
rad

yleft = z*tan(phi-alpha);                % beam radius with angle phi-
alpha
ym = z*tan(phi);                         % beam radius with angle phi
yright = z*tan(phi+alpha);               % beam radius with angle
phi+alpha

a1 = sqrt(z^2+yleft^2);                  % a1 and a2 - distances from
Pitagora theorm
a2 = sqrt(z^2+yright^2);

z1 = z/cos(phi);                         % new distance with cosine of
rotated angle phi
z2_min = a1*cos(alpha);                  % minimal distance of beam
z2_max = a2*cos(alpha);                  % maximal distance of beam


z2 = linspace(z2_min,z2_max,201);

%% 1) Linear beam radius
```

```
w_z = z * tan(alpha);                       % Constant beam radius in m


w_z1 = z1*tan(alpha);                       % new beam width radius in m
w_z2 = z2.*tan(alpha);                      % vector of beam width radius



%% 2) Total intensity of gaussian distribution in W/m^2

P_t = 0.006*ones(size(z2));
% Total power in Watt of a light source



r = linspace(-0.01,0.01,201);
x=linspace(-0.003, 0.003,12);


I_0 = 2*P_tx/(pi*(w_z)^2);
% Maximal intensity of gaussian in distribution in W/m^2
I_gauss = I_0*exp((-2*(r.^2)/(w_z^2)));
% Total intensity of normal gaussian distribution in W/m^2

I_00 = 2*P_t./(pi*(w_z2).^2);
% Maximal intensity of phase shifted gaussian in distribution in W/m^2

%% First example

I_gauss1 = I_00.*exp((-2*(r-x(1,3)).^2)/(w_z1^2));
% Total intensity of  gaussian distribution in W/m^2
I_gauss2 = I_00.*exp((-2*(r-x(1,10)).^2)/(w_z1^2));
I_gauss3 = I_00.*exp((-2*(r-x(1,10)).^2)/(w_z1^2));
I_gauss4 = I_00.*exp((-2*(r-x(1,3)).^2)/(w_z1^2));
I_gauss5 = I_00.*exp((-2*(r-x(1,4)).^2)/(w_z1^2));
I_gauss6 = I_00.*exp((-2*(r-x(1,2)).^2)/(w_z1^2));
I_gauss7 = I_00.*exp((-2*(r-x(1,1)).^2)/(w_z1^2));
I_gauss8 = I_00.*exp((-2*(r-x(1,12)).^2)/(w_z1^2));
Ig1 =
I_gauss1+I_gauss2+I_gauss3+I_gauss4+I_gauss5+I_gauss6+I_gauss7+I_gauss
8;

%% Second example
I_gauss1 = I_00.*exp((-2*(r-x(1,12)).^2)/(w_z1^2));
% Total intensity of  gaussian distribution in W/m^2
I_gauss2 = I_00.*exp((-2*(r-x(1,8)).^2)/(w_z1^2));
I_gauss3 = I_00.*exp((-2*(r-x(1,6)).^2)/(w_z1^2));
I_gauss4 = I_00.*exp((-2*(r-x(1,2)).^2)/(w_z1^2));
I_gauss5 = I_00.*exp((-2*(r-x(1,4)).^2)/(w_z1^2));
I_gauss6 = I_00.*exp((-2*(r-x(1,12)).^2)/(w_z1^2));
I_gauss7 = I_00.*exp((-2*(r-x(1,12)).^2)/(w_z1^2));
I_gauss8 = I_00.*exp((-2*(r-x(1,12)).^2)/(w_z1^2));
Ig2 =
I_gauss1+I_gauss2+I_gauss3+I_gauss4+I_gauss5+I_gauss6+I_gauss7+I_gauss
8;

%% Third example
```

```
I_gauss1 = I_00.*exp((-2*(r-x(1,3)).^2)/(w_z1^2));
% Total intensity of  gaussian distribution in W/m^2
I_gauss2 = I_00.*exp((-2*(r-x(1,9)).^2)/(w_z1^2));
I_gauss3 = I_00.*exp((-2*(r-x(1,12)).^2)/(w_z1^2));
I_gauss4 = I_00.*exp((-2*(r-x(1,4)).^2)/(w_z1^2));
I_gauss5 = I_00.*exp((-2*(r-x(1,6)).^2)/(w_z1^2));
I_gauss6 = I_00.*exp((-2*(r-x(1,2)).^2)/(w_z1^2));
I_gauss7 = I_00.*exp((-2*(r-x(1,10)).^2)/(w_z1^2));
I_gauss8 = I_00.*exp((-2*(r-x(1,12)).^2)/(w_z1^2));
Ig3 =
I_gauss1+I_gauss2+I_gauss3+I_gauss4+I_gauss5+I_gauss6+I_gauss7+I_gauss
8;



%% Graph

figure
subplot(4,1,1)
plot(r,I_gauss,'k.','MarkerSize',10);
title('Normal Gaussian beam','FontWeight','bold');
xlabel('Distance in m');
ylabel('GB distribtion intensity');
legend ('Intensity in W/m^2');
grid on
subplot(4,1,2)
plot(r,Ig1,'k.','MarkerSize',10,'Color','red');
title( 'Beam distribution with 8 optical
sources','FontWeight','bold');
xlabel('Distance in m');
ylabel('Beam distribtion intensity');
legend ('Intensity in W/m^2');
grid on
subplot(4,1,3)
plot(r,Ig2,'k.','MarkerSize',10,'Color','blue');
title( 'Beam distribution with 8 optical
sources','FontWeight','bold');
xlabel('Distance in m');
ylabel('Beam distribtion intensity');
legend ('Intensity in W/m^2');
grid on
subplot(4,1,4)
plot(r,Ig3,'k.','MarkerSize',10,'Color','green');
title( 'Beam distribution with 8 optical
sources','FontWeight','bold');
xlabel('Distance in m');
ylabel('Beam distribtion intensity');
legend ('Intensity in W/m^2');
grid on
```